



UNIVERSIDADE D
COIMBRA

Ana Luísa Gomes da Silva

ACTIVE POWER STORAGE USING 3D LI-ION BASED
THIN FILM CATHODES: A NOVEL SPUTTERING
TECHNOLOGY APPROACH

ARMAZENAMENTO ACTIVO DE ENERGIA UTILIZANDO CÁTODOS 3D DE FILME
FINO À BASE DE IÕES DE LÍCIO: UMA NOVA ABORDAGEM POR TECNOLOGIA DE
PULVERIZAÇÃO

Dissertação de Mestrado em Engenharia do Ambiente, na área de Especialização
em Tecnologia e Indústria Sustentável, orientada pela Professora Doutora Sandra
Maria Fernandes Carvalho e pela Doutora Cristiana Filipa Almeida Alves e
apresentada ao Departamento de Engenharia Civil da Faculdade de Ciências e
Tecnologia da Universidade de Coimbra

Maio de 2023

Faculdade de Ciências e Tecnologia da Universidade de Coimbra
Departamento de Engenharia Civil

Ana Luísa Gomes da Silva

ACTIVE POWER STORAGE USING 3D LI-ION BASED THIN FILM CATHODES: A NOVEL SPUTTERING TECHNOLOGY APPROACH

ARMAZENAMENTO ACTIVO DE ENERGIA UTILIZANDO CÁTODOS 3D DE FILME FINO À BASE DE IÕES DE LÍTIO: UMA NOVA ABORDAGEM POR TECNOLOGIA DE PULVERIZAÇÃO

Dissertação de Mestrado em Engenharia do Ambiente, na área de Especialização em Tecnologia e Indústria Sustentável,
orientada pela Professora Doutora Sandra Maria Fernandes Carvalho e pela Doutora Cristiana Filipa Almeida Alves.

Esta Dissertação é da exclusiva responsabilidade do seu autor. O Departamento de Engenharia Civil da FCTUC
declina qualquer responsabilidade, legal ou outra, em relação a erros ou omissões que possa conter.

Maio de 2023



UNIVERSIDADE D
COIMBRA

AGRADECIMENTOS

À Professora Sandra e à Cristiana, por toda a dedicação, paciência, persistência, sacrifício e compreensão ao longo dos percalços da minha dissertação.

Ao IPN, ao DEM e a todos que contribuíram para que este trabalho fosse possível.

Aos meus colegas, chefe do DMAS e diretor do SGIP pela confiança e flexibilidade que me permitiu estar a estagiar e a realizar a dissertação de mestrado em simultâneo.

Ao NEEA/AAC, a quem o constitui e constituiu, às pessoas maravilhosas que conheci antes e durante a minha vida académica e em especial às que mantenho amizade, pelos momentos e experiências que me proporcionaram e que guardo com carinho.

Ao Bernardo pela paciência, apoio e amor incondicional.

Às minhas famílias de sangue e emprestada, pilares da minha estabilidade, pelo apoio, carinho e compreensão com que me brindaram ao longo da minha vida.

Aos meus pais, nunca algum agradecimento será suficiente. Fizeram tudo ao seu alcance para me ajudar a atingir todos os meus objetivos e ver-me feliz. A eles devo a pessoa que sou, o meu percurso, este trabalho e este especial agradecimento.

A todos, do fundo meu coração, obrigada por tudo!

RESUMO

As alterações climáticas são um problema global conhecido que afeta a qualidade de vida da população, tornando clara a necessidade de alcançar uma gestão sustentável e uma utilização eficiente dos recursos naturais. As baterias de íões de lítio (LIBs) são cruciais para o armazenamento de energia, em particular para aplicações móveis e micro/nano-eletrónicas, Internet das Coisas (IoT), fotovoltaica (PV) e dispositivos biomédicos. Contudo, nas LIB comerciais, os materiais catódicos apresentam heterogeneidades na composição química e estrutura cristalina, impedindo assim que os materiais exibam toda a sua densidade de energia.

Devido à dependência energética e à diminuição dos materiais disponíveis, é necessário desenvolver novas soluções para o armazenamento de energia. Isto leva ao interesse do estudo de baterias de filme fino por pulverização magnética, uma tecnologia limpa e segura que permite reduzir a quantidade de materiais necessários.

Óxido de lítio cobalto (LiCoO_2), foi um dos primeiros cátodos utilizados em baterias. Assim, foi desenvolvido um filme fino de LiCoO_2 para representar um cátodo tradicional e um filme fino de carbono do tipo diamante (DLC) para representar um ânodo.

Neste sentido, o trabalho interdisciplinar abrangeu a deposição de dois filmes finos: LiCoO_2 e DLC tendo sido obtidos revestimentos com 40 nm e 260 nm de espessura, determinada por AFM e SEM, respetivamente. O objetivo desta abordagem foi comparar o potencial de ambos os revestimentos num ambiente similar ao de uma bateria. Para além da deposição dos filmes finos foi realizada também a análise e caracterização do comportamento eletroquímico de ambos.

Com esta dissertação, foi possível concluir por XRD que ambos os revestimentos têm uma estrutura amorfa. Através da PP e EIS, foi possível concluir também que ambos os filmes têm uma boa taxa de corrosão e são corroídos numa só constante.

Palavras-chave: Baterias, Lítio, NMC, Filmes finos, Caracterização eletroquímica

ABSTRACT

Climate change is a global problem known to affect population life quality, making clear the necessity to achieve sustainable management and efficient use of natural resources. Among these, Li-ion batteries (LIBs) are crucial for energy storage, in particular for mobile and micro/nano-electronics applications, Internet of Things (IoT), photovoltaics (PV) and biomedical devices. Yet, in commercial LIBs, the cathode materials exhibit chemical composition and structural heterogeneities, thus preventing materials from exhibiting their full energy-density.

Due to the energy dependency and depletion of materials its necessary to develop new solutions for energy storage. This leads to the interest of studying thin film batteries by magnetron sputtering, a clean and safe technology that allows to reduce the amount of materials need.

Lithium cobalt oxide (LiCoO_2) was one of the first cathodes used in batteries. Thus, a LiCoO_2 thin film was developed to represent a traditional cathode and a diamond-like carbon (DLC) thin film to represent an anode.

In this sense, the interdisciplinary work covered the deposition of two thin films: LiCoO_2 and DLC, obtaining coatings with 40 nm and 260 nm thickness, determined by AFM and SEM, respectively. The aim of this approach was to compare the potential of both coatings in a battery-like environment. Besides the deposition of the thin films, the electrochemical behaviour of both coatings was also analysed and characterised.

With this dissertation, it was possible to conclude by XRD that both coatings have an amorphous structure. Through PP and EIS, it was also possible to conclude that both films have a good corrosion rate and are corroded in one constant.

Keywords: Batteries, Lithium, NMC, Thin Films, Electrochemical Characterization

INDEX

AGRADECIMENTOS	i
RESUMO	ii
ABSTRACT	iii
FIGURE INDEX	vi
TABLE INDEX	viii
ABBREVIATIONS	ix
SIMBOLOGY	xi
1 INTRODUCTION	1
1.1 Motivation	1
1.2 Goals	2
1.3 Organisation and structure of the document	3
2 STATE OF THE ART	4
2.1 Energy Paradigm: Current Challenges	4
2.2 Li-ion batteries	8
2.2.1 Battery Operations	10
2.2.2 Materials used	11
2.2.3 LiNiCoMnO ₂ (NMC) Batteries	15
2.3 Solid state batteries	16
2.4 Thin film batteries	17
2.5 Applications in microelectronics	19
3 MATERIALS AND METHODS	22
3.1 Introduction	22
3.2 Sputtering deposition	22
3.3 Experimental details of LiCoO ₂ deposition	25
3.4 Experimental details of Carbon deposition	26
3.5 Characterization techniques	26
3.5.1 Scanning electron microscopy and energy dispersive X-ray spectroscopy	26

3.5.2	X-Ray Diffraction	27
3.5.3	Atomic force microscopy	27
3.5.4	Potentiodynamic polarization and Electrochemical impedance spectroscopy	28
4	RESULTS	30
4.1	Introduction	30
4.2	Chemical composition and surface characterization	30
4.3	Structural characterisation	33
4.4	Electrochemical performance	35
5	CONCLUSIONS AND FUTURE WORK	46
5.1	Conclusions	46
5.2	Notes and potentially useful elements	47
	BIBLIOGRAPHIC REFERENCES	48

FIGURE INDEX

Figure 2.1 Thermal-power energy and losses in the production of one unit of useful light energy (Boko et al., 2007).	4
Figure 2.2 Lithium Production and Reserves (<i>USGS.Gov / Science for a Changing World</i> , 2010).	7
Figure 2.3 Components of a rechargeable Li-ion battery (Goodenough, 2018).	11
Figure 2.4 Comparison of energy density of lithium cells and other types of cells (Crompton, 1996).	13
Figure 2.5 Snapshot of NMC (Buchmann, 2019).	16
Figure 2.6 Schematic cross section of a thin film battery fabricated by vapor deposition onto both sides of a substrate support (Dudney, 2013).	17
Figure 2.7 Thin film battery schematic illustration. The arrows represent the discharge reaction, in which a Li ion diffuses from the lithium metal anode to fill a space in an intercalation compound that acts as the cathode. The compensating electron travels through the device (Dudney, 2013).	18
Figure 2.8 Examples of lithium battery applications and the form of cells used (Yuxing Wang et al., 2015b).	21
Figure 3.1 Plasma process inside the chamber (<i>Chapter 11 - Bioactive Surface Coatings for Enhancing Osseointegration of Dental Implants</i> , 2019)	23
Figure 3.2 Direct Current Magnetron Sputtering system.	24
Figure 3.3 Schematic representation of de DC MS system.	25
Figure 3.4 AFM schematic	28
Figure 4.1 Cross section by SEM of DLC film	31
Figure 4.2 Thickness of LiCoO ₂ film by AFM	31
Figure 4.3 Surface of DLC film by SEM	32
Figure 4.4 Surface of LiCoO ₂ film by SEM.	32
Figure 4.5 AFM of LiCoO ₂ film.	33
Figure 4.6 X-Ray diffractogram of LiCoO ₂ coating.	34
Figure 4.7 X-Ray diffractogram of DLC coating	34
Figure 4.8 Polarization curves of DLC and LiCO ₂ coatings.	35
Figure 4.9 Pourbaix diagram of Li	37
Figure 4.10 Pourbaix diagram of Co	38
Figure 4.11 Pourbaix diagram of C	39
Figure 4.12 Bode and phase angle plots of LiCoO ₂ as an anode.	40
Figure 4.13 Bode and phase angle plots of LiCoO ₂ as a cathode.	40
Figure 4.14 Bode and phase angle plots of DLC as a cathode	41
Figure 4.15 Bode and phase angle plots of DLC as an anode.	41

Figure 4.16 Nyquist plots of LiCoO_2	42
Figure 4.17 Nyquist plots of DLC	42
Figure 4.18 Equivalent electrical circuit to DLC film.....	44
Figure 4.19 Equivalent electrical circuit to LiCoO_2 when it behaves like an anode.....	44
Figure 4.20 Equivalent electrical circuit to LiCoO_2 when it behaves like a cathode.....	45

TABLE INDEX

Table 2.1 Features of energy storage technologies (Zablocki, 2019).....	6
Table 2.2 World Lithium Reserves (<i>USGS.Gov / Science for a Changing World</i> , 2010).....	7
Table 2.3 Various rechargeable lithium metal battery systems developed (Yoshio et al., 2009).	10
Table 2.4 Characteristics and properties of Li-ion battery using various chemistries (Blomgren, 2017; Buchmann, 2019; A. I. Stan et al., 2014).....	14
Table 3.1 Initial parameters of the Magnetron Sputtering system of LiCoO ₂ deposition.	25
Table 3.2 Potentiodynamic scans parameters.....	29
Table 4.1 Chemical composition of LiCoO ₂ coating.	33
Table 4.2 Fit parameters of polarization potentiodynamic curves from samples in 1M of NaOH solution.....	36
Table 4.3 Fit parameters of EIS of DLC according to the equivalent electric circuit.	43

ABBREVIATIONS

3D	Three Dimensional
AFM	Atomic Force Microscopy
CPE	Constant Phase Element
DC	Direct Current
DC-MS	Direct Current Magnetron Sputtering
DLC	Diamond-Like-Carbon
EDS	Energy Dispersive Spectroscopy
EEC	Equivalent Electric Circuit
EIS	Electrochemical Impedance Spectroscopy
ESD	Electrostatic-spray Deposition
EU	European Union
GHG	Greenhouse Gases
IoT	Internet of Things
IPN	Instituto Pedro Nunes
LIB	Lithium-Ion Batteries
MEMs	Micro-Electromechanical Systems
MS	Magnetron Sputtering
OCP	Open Circuit Potential
PLD	Pulsed Laser Deposition
PP	Polarization Potentiodynamic

PV	Photovoltaics
PVD	Physical Vapor Deposition
RFID	Radio-Frequency Identification
SEI	Solid Electrolyte Interphase
SEM	Scanning Electron Microscope
TFB	Thin-film Lithium Battery
UPS	Uninterruptible Power Supplies
US	United States
XRD	X-Ray Diffraction

SIMBOLOGY

Ar	Argon
C	Carbon
C ₂ H ₆ O	Ethanol
C ₃ H ₆ O	Acetone
Co	Cobalt
C _{film}	Capacitance of the film
C _{pore}	Capacitance of the pores
E _{corr}	Corrosion Potential
I _{corr}	Corrosion Rate
J _{corr}	Current Density
Li	Lithium
Li ₂ TiO ₃ – LTO	Lithium Titanate
LiCoO ₂ – LCO	Lithium Cobalt Oxide
LiFePO ₄ – LFP	Lithium Iron Phosphate
Li-ion	Lithium-Ion
LiMn ₂ O ₄ -LMO	Lithium Manganese Oxide
LiNiCoMnO ₂ – NCM	Lithium Nickel Manganese Cobalt Oxide
MoS ₂	Molybdenum Disulphide
Na-NiCl ₂	Zebra Batteries
NaS	Sodium-sulfur

NiCd	Nickel-cadmium
Ni-MH	Nickel-hydride
NMC	Nickel Manganese Cobalt
Pb-acid	Lead Acid
R_{film}	Resistance of the coating
R_{liq}	Resistance of the electrolyte
R_{pore}	Resistance of the pores
Si	Silicon
β_a	Anodic Slopes
β_c	Cathodic Slopes
TiS ₂	Titanium Disulphide

1 INTRODUCTION

1.1 Motivation

According to the European Commission, energy production and consumption account for more than 75% of the European Union's (EU's) greenhouse gas emissions. The European Commission has established the European Green Deal: a package of legislative recommendations to the EU's climate, energy, transportation, and taxation policies (Parliament, 2020).

These policies were established with the purpose of achieve a 55% decrease in net greenhouse gas emissions by 2030 compared to 1990 levels, such as 32% of energy from renewable sources in gross final consumption, a reduction of 32.5% in energy consumption, a reduction in greenhouse gas emissions of 40% and an increase in electricity interconnections of 15%.

To fulfil the 2030 climate targets and the EU's long-term goal of carbon neutrality by 2050, is imperative to decarbonize the EU's energy sector. The European Green Pact remains the European Commission's top long-term goal, as it was both during the 19-covid pandemic and Russia's invasion of Ukraine. The entire situation, including the rise in inflation has contributed to the increase in the cost of living leading to motivate people to reduce their energy consumption for reasons other than environmental ones.

The availability of renewable resources is not constant, as is the case with fossil resources. Both wind and solar energy are completely dependent on the natural resources existing in the environment in which they are located. Wind speed is not constant throughout the day, just as at night there is no radiation available to supply the solar panels. This instability of production makes it impossible to consider the independence acquired from renewable sources in relation to the ones obtained from fossil resources.

In this regard, energy storage is a crucial part of this new sustainable energy paradigm, which is heavily reliant on renewable energies and on self-production like micro-generation (generating electricity to sell on a small-scale). It allows for the solution of the high degree of intermittency of renewable energy sources by storing it during off-peak hours to be used later during peak hours, when resources, such as sun and wind, are scarce or unavailable.

Electrochemical and battery, thermal, thermochemical, flywheel, compressed air, pumped, magnetic, chemical and hydrogen energy storage systems are the most common types of energy storage (Breeze, 2014).

Batteries are highly developed energy storage devices with high energy densities and voltages. There are several types of batteries, including lithium-ion (Li-ion), sodium-sulphur (NaS), nickel-cadmium (NiCd), lead acid (Pb-acid), lead-carbon, zebra batteries (Na-NiCl₂), and flow batteries. All batteries have one thing in common: they run for a while, need to be recharged, and eventually need to be replaced when their capacity depletes. Battery research is progressing quickly, indicating that the “Super Battery” has not yet been discovered but may be just around the corner. Particularly, Li-ion is expensive, but when the price per cycle is calculated, it outperforms lead acid when repeat cycling is required (Breeze, 2014).

Currently, the subject of energy is a constant in daily lives, not only because the bill to pay at the end of the month but also because the dependency on energy for practically all the routine tasks. This energy dependency has intensified with the exponential evolution of technology, making it unsustainable for society, economy, and environment.

The need to develop “cleaner” technologies with less impact on the environment lead to the increase of investigations on alternatives to energy sources for renewables, efficient energy storage solutions and, more recently, on the alternatives and reduction of materials to increase the sustainability of these solutions.

Thus, we are currently witnessing the transition from the petroleum era to the rare metal’s era. Rare earth metals are the critical raw materials need to decarbonise our economy and promote the EU’s energy transition towards green technologies.

The energy model transition is not just about changes in energy technologies and sources, it is about a paradigm shift in policies, models, infrastructures, systems, technologies, and sources of energy and, above all, in people’s behaviour.

1.2 Goals

One of the initial objectives of this dissertation was to explore the current situation of energy and batteries, as well as to learn several types of existing solutions and their advantages and disadvantages.

The main objective of this dissertation was to learn what sputtering deposition is as well as its environmental benefits and the various existing electrochemical characterization technologies.

The main goal of this project was to deposit two thin films (LiCoO₂ and DLC) and simulate and compare the potential of both coatings in a similar working environment of a battery.

1.3 Organisation and structure of the document

This master's thesis is divided into five chapters and a bibliography. The first chapter is an introduction to the topic being discussed, setting the subject in context, presenting the motivation and goals for conducting the current thesis, as well as its organisation and structure.

The second chapter discusses the State of the art in terms of the current challenges of energy storage and more specifically Li-ion batteries as well as their operations and types of cathode materials used. LiNiCoMnO_2 (NMC) cathode battery materials are presented and the importance of cobalt amount reduction. Furthermore, future batteries such as solid-state batteries and thin film batteries are introduced and in addition their applications in smaller batteries.

In the third chapter, the parameters, machines, and methods utilised for all the experiments are presented, as well as the explanation of the processes of the techniques used.

The experimental results are presented in the fourth chapter and lastly the conclusions are presented in the final chapter with reference to the results obtained and future research opportunities.

2 STATE OF THE ART

2.1 Energy Paradigm: Current Challenges

Energy is the ability to produce work and has its origin in two types of energy sources: renewable and non-renewable. Renewable energy sources come directly from nature and renew through endless natural cycles such as water, biomass, geothermal, waves, solar radiation, or wind. Non-renewable energy sources are limited resources, which are depleted as they are used, and which are dependent on the planet's existing resources or their rate of renewal like fossil fuels (coal, oil, and natural gas). The final energy that is received in houses refer to the total of energy produced (primary energy) without the total losses of energy during the processes of transformation and the sequence of energy lost in transport, distribution, and storage. Furthermore, the equipment used has an efficiency that will provide the energy truly used (useful energy) (Administration et al., 2023). The Figure 2.1 shows how the conversion from primary energy to end-uses has an extremely low efficiency.

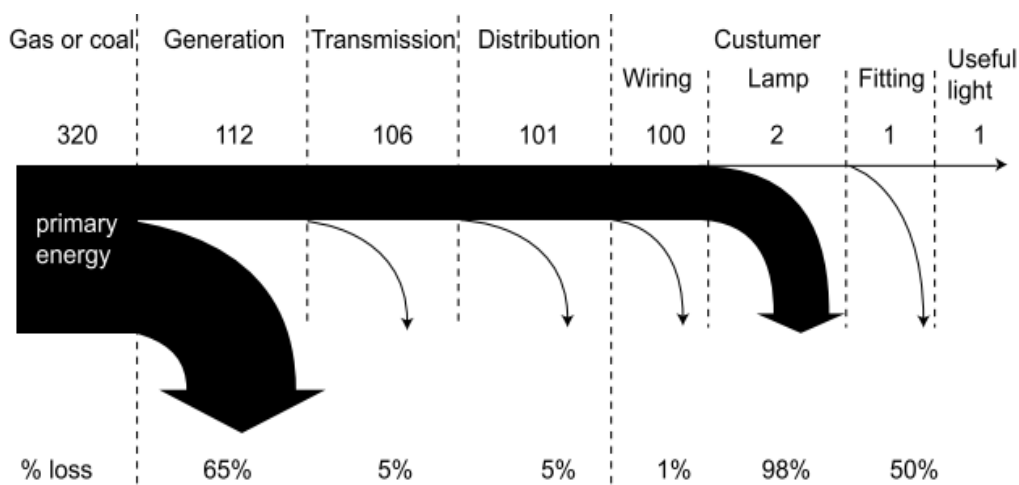


Figure 2.1 Thermal-power energy and losses in the production of one unit of useful light energy (Boko et al., 2007).

Energy use and production set significant pressures on the environment because non-renewable fuels are used to supply about 80 percent of the world's energy and a considerable part of this energy is wasted before and during use (Boko et al., 2007).

Fossil fuels are formed by a slow process of decomposition of buried carbon-based organisms that died millions of years ago. When fossil fuels burn, they release carbon dioxide and other greenhouse gases, which trap heat in our atmosphere, making them the principal contributors to global warming and climate change (Botto, 2007; Yildiz, 2018).

Modern society is dependent on energy and fossil fuels. However, issues like unaffordable prices, security of supply, inflation, depletion, and changes in the environment caused by the exploration and use of fossil resources, highlight the urgency of reflecting on current energy challenges (IEA, 2022).

The management of energy resources must focus on saving and efficiently use energy while reducing dependence on fossil fuels and replacing them with “clean energy”. The expression could have a positive connotation but, far from it, the transition to renewables is requiring a dramatic increase of extraction of metals and rare-earth minerals, causing ecological and social costs (Holechek et al., 2022).

Although, theoretically, hydrogen-based renewable energy storage is more dependable and effective than conventional battery-based energy storage, energy storage in hydrogen has a problem in terms of its low efficiency in the electricity-hydrogen-electricity conversion process, in addition to the fact that, economically, it cannot yet compete with battery storage (Bernal-Agustín & Dufo-López, 2009) .

Energetic systems can facilitate the transition for a decarbonized electrical system because it allows flexible production of renewable energy and guarantees its integration into the system. Consequently, is one of the key elements to deliver future energy needs at low/zero GHG emissions levels (Martins et al., 2022).

Energy storage allows the energy-supply system to operate independently from the energy-demand system. It allows us to use energy supplies when short-term demand does not exist, to respond to brief-term fluctuations in demand and to recover wasted energy. Storage is essential to low-carbon energy options to better use in terms of efficiencies and thus emissions. However, the cost and durability of the high-technology systems continues to be a big challenge (Boko et al., 2007).

Storage batteries represent a promising solution to fill the disparity in storage needs for the future, because they can provide an important connection between the primary source of energy and its actual use, corresponding with demand in intermittent energy systems and offer the possibility to choose better options for the primary energy sources. Nowadays there is available several technologies for storage, conversion, and use of thermal, mechanical, chemical, electrical, and magnetic energy (Zablocki, 2019). Table 2.1 lists some features of energy storage technologies.

The specific energy of energy storage technologies is Important for electric vehicle applications and energy/land area ratio and efficiency necessary for utility load-levelling

applications. The higher these values are, the more useful they will be to the mentioned applications (Zablocki, 2019).

However, advanced batteries with high specific energy, high specific power, durability, and low cost must be developed to permit technologies like electric vehicles and load levelling devices to compete (Zablocki, 2019).

Currently, the most battery systems used are the rechargeable lead acid and the primary manganese dioxide-zinc. However, LIB has a low atomic number and a high electrode potential that results in significantly high-energy density, reliable performance, and no memory effect as occurred with nickel-cadmium (Ni-Cd) or nickel-hydride (Ni-MH) batteries compared to lead and zinc in the traditional batteries. LIBs have been used essentially for portable electronics (Yoshio et al., 2009).

Table 2.1 Features of energy storage technologies (Zablocki, 2019).

Energy storage system	Specific energy (Wh/kg)	Energy/area ratio (kWh/m ²)	Efficiency (%)	Cost ^a (\$/kW)
Batteries	40–100	40–80	70–85	600–1100
Thermal	—	—	60–90	600–700
Pumped hydro	—	—	70	700–900
Compressed air	—	—	70–85	500–600
Flywheels	10–20	—	70	1600–3200
Hydrogen	80	—	50–60	>1000
Magnetic	—	—	90	1000–1800

^a 5–10-hour discharge duration

Despite the primary appraisal metric of storage batteries being the standardized energy cost, LIBs studies are focused on pushing the performance limits of electrodes and electrolytes for an ever-higher energy density (He et al., 2021).

Lithium consumption for batteries increased dramatically in recent years because of rechargeable lithium batteries and ceramics and glass applications. Figure 2.2 and Table 2.2 shows, according to the US Geological Survey, that Chile, China, Argentina, and Australia have the leading reserves of lithium in the world, with Portugal having reserves of 60 000 ton (*USGS.Gov / Science for a Changing World*, 2010).

Thus, to be able to deliver on a carbon-constrained future, the metals that are likely to grow in demand are aluminium, cobalt, copper, iron ore, lead, lithium, nickel, manganese, the

platinum group of metals, rare earth metals, silver, steel, titanium, and zinc (“Grow. Role Miner. Met. a Low Carbon Futur.,” 2017).

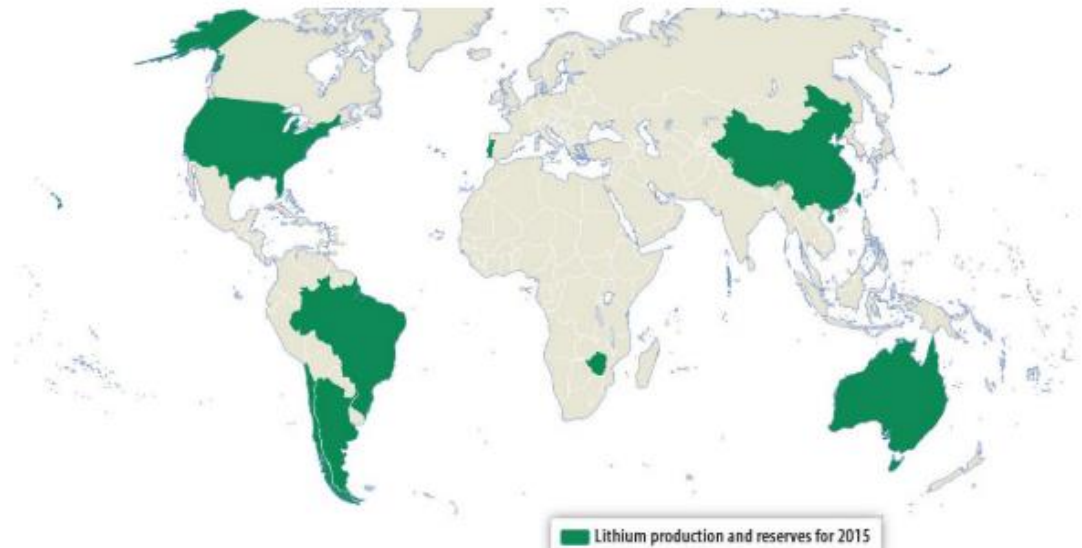


Figure 2.2 Lithium Production and Reserves (*USGS.Gov | Science for a Changing World, 2010*).

Table 2.2 World Lithium Reserves (*USGS.Gov | Science for a Changing World, 2010*).

Countries	Reserves (tons)
Unites States	750 000
Argentina	2 200 000
Australia	5 700 000
Brazil	95 000
Chile	9 200 000
China	1 500 000
Portugal	60 000
Zimbabwe	220 000
Other Countries	2 700 000
World total (rounded)	22 000 000

Particularly for lithium-ion batteries, future metal demand is heavily dependent on total demand for storage in the energy system, the choice of energy storage technologies, and the development of less-metal-demanding technologies (Mikael Hanicke, Dina Ibrahim, Sören Jautelat, Martin Linder, Patrick Schaufuss, Lukas Torscht, 2023).

The lithium debate is diverging. On one hand, the possible profit in long term in a new energy source that replaces the paradigm of carbon and fossil sources. On the other hand, because of

lithium operations the possible destruction of the environment, contamination of rivers, destruction of mountains, mine open skies and ending the sustainable tourism (Marco Tedesco, 2023).

2.2 Li-ion batteries

A battery or an electrochemical cell is a device that allows the energy liberated in a chemical reaction converted to electricity (Dr Anand Bhatt, 2016).

Nowadays is almost universally accepted that Luigi Galvani and Alessandro Volta at the end of the eighteenth century created for the first time an electrochemical cell. The two scientists had a dispute about the classic experiment where a frog's leg spasm when touched by a series of two different metals. While Galvani said that animals could generate electricity, Volta argued his point by the demonstration of electricity production from his "voltaic pile" formed by an alternate sequence of two different metals (Scrosati, 2011).

Volta started a series of experiments using zinc, lead, tin, and iron as cathodes, and copper, silver, gold, and graphite as anodes. In 1800, Volta found that certain fluids when used as a conductor would generate a continuous flow of electrical power. This discovery led to the invention of the first voltaic cell, better known as a battery. Volta discovered after that when voltaic cells were stacked on top of each other the voltage would increase. Volta's work had a huge impact on the progress of the electrochemical science by stimulating a rapid evolution of the battery history and the discoveries of many important electrochemical systems (Scrosati, 2011).

The discoveries of a battery based on a zinc rod negative electrode (anode) and a manganese oxide-carbon mixture as positive electrode (cathode) immersed in an aqueous ammonium chloride solution by Georges-Lionel Leclanché in 1866, the lead-acid rechargeable battery by Gaston Planté in 1859 and the rechargeable nickel-cadmium battery by Waldmar Jungner in 1901, pleased the needs of the time. But the succession of innovations in the late 1960s such as the implantable medical devices, the request of high-energy and high-power sources for military purposes, and the explosion of the consumer electronic market demanded portable energy (Scrosati, 2011).

The lack the energy density associated with the electrode combination that offers only a limited value of specific capacity reflects a low energy density in the conventional batteries. Furthermore, these batteries were too heavy and too big to satisfactorily serve the evolving technology. In that time, there was an urgent need for a new battery with higher energy-to-weight and energy-to-volume ratio, combined with a long operational life. The discovery of a new concept batteries with lithium as one of the electrode materials ensured a theoretical

specific capacity significantly higher than zinc. Its use required moving from the common aqueous electrolytes to more electrochemically stable organic electrolytes, formed by a solution of lithium salt in a carbonate organic solvent or in a mixture of them, because of the lithium metal incompatibility with water (Scrosati, 2011).

A lithium–iodine battery provided an energy density almost five times higher than zinc–mercury oxide. This replacement resulted in considerable reduction of weight and volume extending the operational life to 6 or 7 years. The enormous success of the lithium–iodine battery emphasised the potentiality and opened the possibility to develop a series of new batteries capable of meeting the various requests and applications. In the 1970s, the electronics brought into the market like electronic watches, toys, and cameras required batteries capable of providing a good powering operation with a small volume size and a contained price. To satisfy this need they utilized a primary lithium battery with a manganese dioxide cathode. The success in these batteries boosted the interest in the study of secondary, rechargeable systems and escalated in 1978, with the progress on the “insertion” or “intercalation” electrodes based in compounds that can reversibly accept and release lithium ions (Scrosati, 2011).

The firsts rechargeable lithium batteries arrived in the late 1970s to early 1980s, both using liquid organic electrolytes, one with a TiS_2 cathode and the other with a MoS_2 cathode. Still, these pioneers’ batteries had glitches, such as fire incidents, associated with the anode’s high reactivity. The reaction of lithium metal with the electrolyte forms a layer on its surface, commonly referred as solid electrolyte interphase (SEI), permeable to lithium ions that allows a discharge process. Nevertheless, irregularities on the SEI surface can lead to an additional charge with dendrite formation that eventually grows to short the cell and in extreme cases overheat with thermal runaway and explode. Therefore, to guarantee cycle life and safety they had to carefully choose the electrolyte system to assure optimised, smooth lithium deposition or replace the lithium metal with a less aggressive anode material (Scrosati, 2011).

To improve the development of rechargeable lithium battery the most evident option was the replacement of the lithium metal with another more reliable electrode, but the chosen approach was the combination of two insertion electrodes, one capable of accepting lithium ions (anode), and the other, capable of releasing lithium ions (cathode). The process was referred as a lithium rocking chair battery, was reversible upon charge and discharge and cyclically repeated. Despite the various existing cathodes materials developed, the majority of the commercial production of lithium rocking chair batteries nowadays still relies on lithium cobalt oxide as cathode. The cathodes are important because they provide lithium ions to guarantee the electrochemical process, as well as to accept them back in a reversible matter to confirm the life of the battery (Scrosati, 2011).

Lithium rocking chair batteries that were renamed as LIB, are nowadays the power sources of choice for a series of portable devices, such as cellular phones, notebooks, and others. Table 2.2 documents the various research and progress of rechargeable lithium metal battery systems (Scrosati, 2011).

The present challenge passes from the intercalation chemistry to novel concepts that may increase safety, assure a drastic reduction in cost, and raise energy density. In order to increase safety, is necessaire to find electrolytes that are more thermally stable and/or inert than the ones currently being used and to reduce costs LiCoO_2 must be replaced with cheaper materials. However, increase energy density on batteries is a difficult task. Nowadays, the focus is on batteries based in electrode combinations that, in theory, guarantee a quantum jump in energy density (Scrosati, 2011).

Table 2.3 Various rechargeable lithium metal battery systems developed (Yoshio et al., 2009).

System	Voltage	Wh/kg	Wh/l	Company
Li/TiS ₂	2.1	130	280	'78 Exxon
LiAl/TiS ₂				'79 Hitachi
Li/LiAlCl ₄ -SO ₂ /C	3.2	63	208	'81–85 Duracell
Li/V ₂ O ₅	1.5	10	40	'89 Tohsiba
Li/NbSe ₃	2.0	95	250	'83–86 Bell Lab
LiAl/Polyaniline	3.0	–	180	'87 Bridgestone
LiAl/Polypyrrolle	3.0	–	180	'89 Kanebo
Li/Al/Polyacene	3.0	–	–	'91 Kanebo/Seiko
Li/MoS ₂	1.8	52	140	'87 MoLi
Li/CDMO(Li _x MnO ₂)	3.0	–	–	'89Sanyo
Li/Li _{0.3} MnO ₂	3.0	50	140	'89 Tadiran
Li/VO _x	3.2	200	300	'90 HydroQuebec

2.2.1 Battery Operations

A battery is an energy storage device that is slow to fill, holds limited capacity and has a defined lifetime. Their working principle consists in converting chemical energy into electrical energy through electrochemical reduction-oxidation reactions (Goodenough, 2018).

As you can see in the

Figure 2.3 a battery contains one or several electrolytic cells (liquid or solid), that provide the means to transfer electrons between two electrodes, the anode, the negative one, that gives up the electrons to the external circuit and is oxidised during the reaction and the cathode, the positive electrode that receives the electrons from the external circuit and is reduced during

the electrochemical reaction. The anode and the cathode are separated by an electrolyte (Goodenough, 2018).

The chemical reaction between the electrodes has an ionic and an electronic component. The electrolyte transports the ionic component inside a cell and forces the electronic component to cross an external circuit. The chemical reaction is reversible in a rechargeable battery (Goodenough, 2018).

Lithium-ion batteries have a positive electrode based of lithium metal oxide, a negative electrode made of porous carbon, and an electrolyte made of a lithium aqueous solution. During the charging process, lithium ions from the positive electrode move through the electrolyte to the negative electrode and deposit between the carbon layers. During the discharge process, the reverse occurs (Goodenough, 2018).

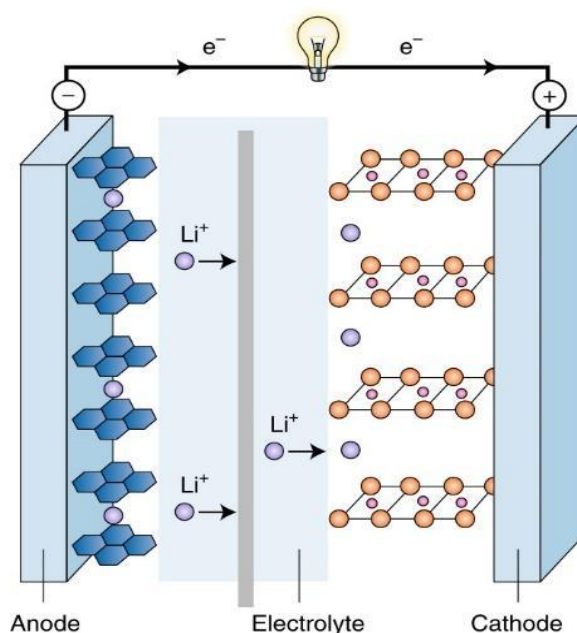


Figure 2.3 Components of a rechargeable Li-ion battery (Goodenough, 2018).

2.2.2 Materials used

There are several types of lithium-ion batteries that share some similarities but differ in chemistry characteristics.

Many high-performance anode materials, including alloy materials, conversion-type transition metal compounds, silicon-based compounds, and carbon-based compounds, have been investigated for potential novel materials for LIB. The first three can have high capacities and high energy densities, exhibit good cycling stability and low irreversible capacity loss.

Nevertheless, they can also have volume changes during cycling, which can lead to mechanical stress and eventual failure of the electrode. Carbon-based compounds have lower capacities compared to other anode materials, however can also have high electronic conductivity and low irreversible capacity loss. (Duan et al., 2023; Nzereogu et al., 2022; Peng et al., 2022)

Particularly, the most common anodes used in LIB and other rechargeable batteries is graphite because of their high capacity, lower operating voltage, good cycling performance and low cost. Diamond-Like-Carbon (DLC) is an example of a carbon coating frequently used because is similar to diamond, so its durable and resistant to wear and corrosion (Duan et al., 2023; Nzereogu et al., 2022; Peng et al., 2022).

In another area of knowledge, Li-cobalt, Li-manganese, NMC and Li-aluminium cathodes are similar in their high capacity and are used in portable applications. Li-phosphate and Li-titanate have lower voltages and have less capacity but are more durable and are used, for example, in portable and stationary energy applications needing high load currents and endurance and in uninterruptible power supplies (UPS), respectively (Buchmann, 2019). The Table 2.3 shows the key characteristics of the batteries listed.

One of the main advantages of lithium-ion batteries is that their lifetime isn't influenced by the number of charge and discharge cycles and their high energy density, instead is influenced by the room and storage temperature and the hermetical seal of the battery (Crompton, 1996).

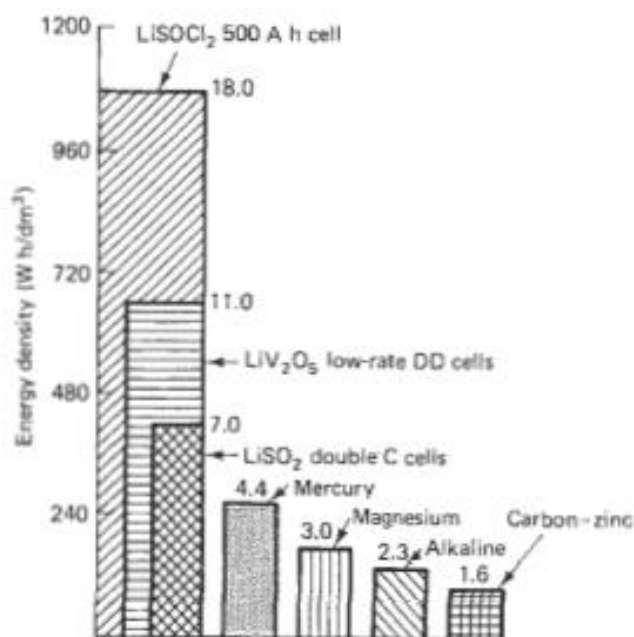


Figure 2.4 Comparison of energy density of lithium cells and other types of cells (Crompton, 1996).

The lithium cobalt oxide (LiCoO_2 — LCO) based battery, is a mature battery technology with a long-life cycle and high energy density. Due to its excellent charging/discharging rate and high energy density, LCO is also the most common battery technology used in portable electronic devices. An anode made of graphite carbon serves as the LC's anode, while the cathode is made of cobalt oxide (A. I. Stan et al., 2014). However, for security reasons and the expensive cost of cobalt, LCO batteries are unsuitable for automotive applications and another issue of LCO-based batteries is their lack of temperature stability (Yixu Wang & Huang, 2011).

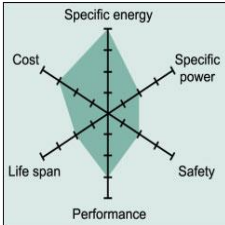
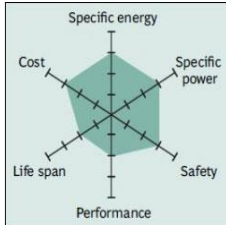
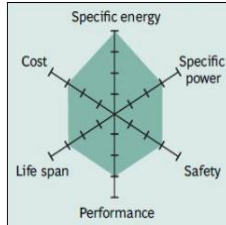
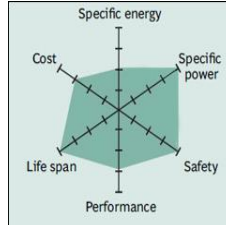
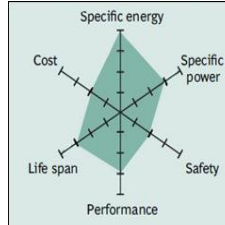
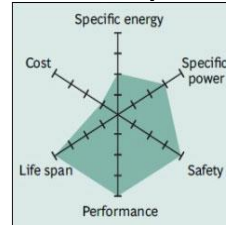
The lithium manganese oxide (LiMn_2O_4 — LMO)-based battery has a nominal voltage rating greater than LCO-based battery cells. However, compared to LCO batteries, the energy density of LMO batteries is around 20% lower. LMO battery cells also have good thermal stability, are less expensive, and have better safety. Even though, the LMO battery cell is not appropriate for electric car, plug-in electric vehicle, or hybrid plug-in electric vehicle applications due to its relatively short life cycle and substantial capacity losses. The power and energy density of LMO batteries are poor (Fergus, 2010; Yixu Wang & Huang, 2011).

Cobalt, nickel, and manganese are the components of the cathode of lithium nickel manganese cobalt oxide, or LiNiMnCoO_2 (NMC). All three transition metals can be presented in equal amounts in the most widely used NMC composition. The capacity, rate, and operating voltage of NMC-based battery cells are all quite high (A.-I. Stan et al., 2014). This topic will be detailed in chapter 2.2.3.

The lithium iron phosphate (LiFePO_4 - LFP) based battery is very appealing due to its large capacity, low cost, flat voltage profile, and minimal environmental impact. Despite having a higher level of safety, LFP batteries operate similarly to NCA batteries. In addition, because of their qualities (high safety, strong thermal stability, long lifetime, and low self-discharge rate), LFP batteries are thought to be suitable for use in stationary, automotive, and backup power applications (Scrosati & Garche, 2010).

In comparison to LCO based batteries, the lithium nickel cobalt aluminium oxide (LiNiCoAlO_2 -NCA) based battery, has a lower voltage and superior safety characteristics. The power density, energy density, and longevity of NCA-based batteries are also good. The poor safety and expensive price of this Li-ion battery chemistry are its principal downsides (Fergus, 2010).

Table 2.4 Characteristics and properties of Li-ion battery using various chemistries (Blomgren, 2017; Buchmann, 2019; A. I. Stan et al., 2014).

	Lithium Cobalt Oxide (LiCoO₂) — LCO	Lithium Manganese Oxide (LiMn₂O₄) — LMO	Lithium Nickel Manganese Cobalt Oxide (LiNiMnCoO₂) — NMC	Lithium Iron Phosphate (LiFePO₄) — LFP	Lithium Nickel Cobalt Aluminium Oxide (LiNiCoAlO₂) — NCA	Lithium Titanate (Li₂TiO₃) — LTO
<i>Specific Capacity [mAh/g]</i>	140	146	145	170	180	170
<i>Nom. Voltage [V]</i>	3.7	3.8	3.6	3.3	3.6	2.2
<i>Energy density [Wh/kg]</i>	110-190	100-120	100-170	90-115	100-150	60-75
<i>Cycle life [cycles]</i>	500-1000	1000	2000-3000	>3000	2000-3000	>5000
<i>Cost [\$/kWh]</i>	48.6	44.5	43.6	50.2	35.0	10.0
<i>Applications</i>	Mobile phones, tablets, laptops, cameras	Power tools, medical devices, electric powertrains	Power tools, medical instruments, e-bikes, EVs.	Portable and stationary needing high load currents and endurance	Medical devices, industrial, electric powertrain (Tesla)	UPS, electric powertrain (Mitsubishi i-MiEV, Honda Fit EV), solar-powered street lighting
<i>Properties</i>	High safety risk, good lifetime	Cheaper, safer than LiCo ₂ and LiNiO ₂	High voltage, good specific capacity, high safety risk, good lifetime	Long lifetime, high stability, basic low cost	High energy, high density, expensive	Negligible volume expansion, basic low cost, stable electrochemical operation, high thermal stability
						

The lithium titanate (Li_2TiO_3 — LTO) based battery have high cycling stability, no electrolyte breakdown (which prevents the production of solid electrolyte interfaces), high rate/discharge capability, and high thermal stability in both charge and discharge state, although their voltage level is lower than that of other Li-ion battery chemistries. Additionally, LTO-based batteries can function in frigid conditions. LTO is also a strong contender for usage in stationery and backup power applications because of those qualities (Yi et al., 2010). Unfortunately, because of the reaction between the organic electrolyte and the LTO active material, LTO suffers from considerable gassing and even with the addition of a carbon coating it can also catalyse and accelerate electrolyte degradation in an SEI, especially at high temperatures (Nitta et al., 2015).

2.2.3 LiNiCoMnO_2 (NMC) Batteries

In what concerns NMC cathode battery materials, it was discovered that adding Co to $\text{Li}(\text{Ni}_{0.5}\text{Mn}_{0.5})\text{O}_2$ represents an effective strategy to further increase the cathode structural stability in comparison to LMO. $\text{LiNi}_x\text{Co}_y\text{Mn}_z\text{O}_2$ has a similar and sometimes greater specific capacity than LCO and a similar operating voltage while having a better cost/benefit ratio due to the lower Co content (Nitta et al., 2015). In this regard, the cathode battery material of many power tool batteries was LCO at first, is now NMC. Consumer electronics applications commonly use NMC due to its easier production methods than NCA and the many cell shapes that can be achieved with this material (Blomgren, 2017).

The most common type of NMC in battery industry was $\text{LiNi}_{0.33}\text{Co}_{0.33}\text{Mn}_{0.33}\text{O}_2$ (Nitta et al., 2015). Although the term "NMC powder" may refer to a mixture, the common composition is 33% nickel, 33% manganese, and 33% cobalt. Due to the lower material cost brought on by the reduction of cobalt percentage, this mix, also known as 1-1-1, is a preferred choice for mass-produced cells in applications requiring frequent (Jung et al., 2020).

The material's adaptability for both high energy and high-power applications has contributed to NMC's rapid development. NMC are now widely available on the market and is the preferred cathode powder for making batteries for electric vehicles such as e-bikes and power tools. It is the top choice for automobile batteries because Ni, Co, and Mn based materials have recently demonstrated it offers better overall performance, excellent specific energy, and the slowest rate of self-heating of any common cathode powder than the other batteries (Jung et al., 2020). Figure 2.5 illustrates these characteristics clearly.

The thermal stability of NMC is one of the major concerns for the battery industry as it is directly related to the battery safety issue especially when cycled at high temperature (Jung et al., 2020).

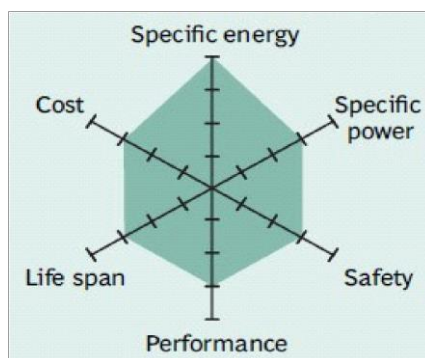


Figure 2.5 Snapshot of NMC (Buchmann, 2019).

2.3 Solid state batteries

The development of lithium-ion batteries and the discovery of fast ionic conduction in solids has stimulated research into solid-state batteries. The non-flammability of their solid electrolytes provides a fundamental solution to safety concerns. These studies have concentrated on the improvement of ionic conductivity because poor ionic conduction in solid electrolytes is a significant drawback in solid-state batteries. Although the studies have identified some high-performance solid electrolytes, some disadvantages have remained hidden until their use in batteries (Takada, 2013).

Solid-state batteries provide potential advantages like no electrolyte leakage, no problems with liquid electrolyte vaporization, no phase transitions at low temperatures, which improves low-temperature performance, and flexibility of downsizing. Also, investigations have demonstrated that solid-state batteries are highly trustworthy, with great storage stability and a very long cycle life (Takada, 2013).

However, recent environmental concerns have increased demand for large-capacity batteries. Batteries are now expected to power cars with efficient energy consumption, and large-scale energy storage becoming necessary to make renewable energy affordable. Yet, as battery size increases, increases the amount of flammable electrolyte. It also improves heat radiation, and the batteries easily heat up to the point of thermal runaway. As a result, increasing battery size aggravates safety concerns. Because of their non-flammability, solid electrolytes are considered to provide a crucial answer to the safety issue. Additionally, compared to consumer batteries, these batteries should have a substantially longer useful life. But, disadvantages such electrolyte impedance, discharge product impedance, and volume fluctuations were identified (Takada, 2013).

Interfacial stability is a key problem for solid-state battery devices (Richards et al., 2016). The application of intercalation chemistry greatly increased battery performance, as evidenced by

lithium-ion batteries with intercalation chemicals on both electrodes. Because intercalation processes do not produce reaction products or cause considerable volume changes, the benefit is significant, especially in solid-state batteries (Takada, 2013).

2.4 Thin film batteries

Thin-film electrode materials could be created by transforming common electrode materials into a thin-film structure and can be prepared using a variety of flexible deposition techniques: magnetron sputtering, pulsed laser deposition (PLD), electron beam evaporation, chemical vapor deposition, electrostatic-spray deposition (ESD), and sol-gel fabrication. Particularly, the magnetron sputtering method produces large-scale, uniform, dense thin films with good adhesion between the film and the substrate (Zhou et al., 2013).

Thin film cathodes are also easily adopted for all-solid-state batteries that do not use a flammable liquid electrolyte and have the advantage that they are free of inactive additives and can be designed to achieve different microstructures or crystalline structures through various thin film techniques (Qi & Wang, 2020).

A thin film battery is made of parallel plates, much like a regular battery, but much thinner. Figure 2.6 represents a thin film battery layout in which films are deposited symmetrically on both sides of a supporting substrate. The entire battery can be flexible when the support is thin, since the entire stack of films is usually around 10 to 15 μm thick and most development is focused on individual cells with active areas with less than 25 cm^2 (Dudney, 2013).

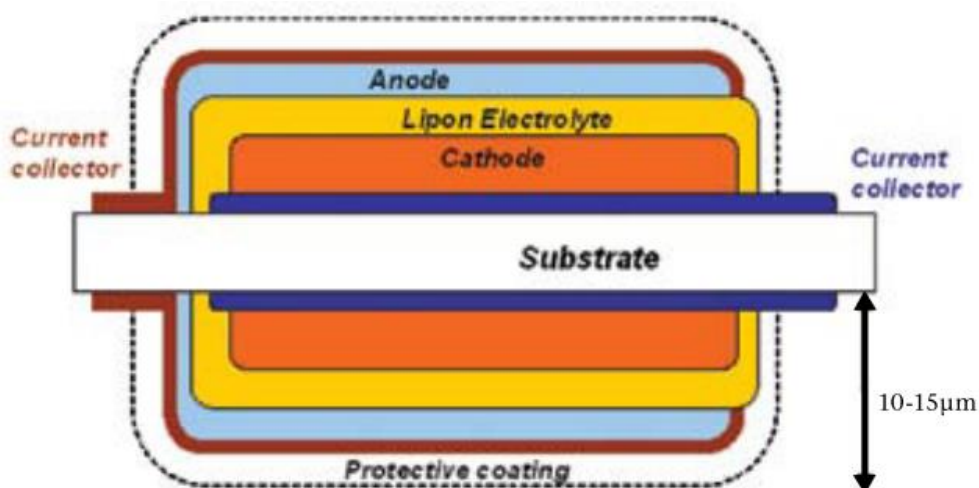


Figure 2.6 Schematic cross section of a thin film battery fabricated by vapor deposition onto both sides of a substrate support (Dudney, 2013).

The operation of a thin film battery is very simple: when the battery is allowed to discharge, a Li^+ ion migrates from the anode to the cathode film by diffusing through the solid electrolyte, (Figure 2.7). The battery can be recharged by reversing the current when the anode and cathode reactions are reversible. The cell voltage is determined by the difference in the electrochemical potential of the lithium (Dudney, 2013).

The most difficult challenges in commercializing thin film battery technology have been supporting the battery on a thin lightweight substrate and protecting the lithium metal and lithium compounds from reaction with gases in the air. To ensure an efficient, lightweight, and affordable packaging, a variety of proprietary packaging materials and battery layouts, such as an inverted stack, are being used (Dudney, 2013).

The most efficient application of thin film batteries is in a fully integrated device. When physically integrated, the materials required to support and protect the thin film battery should serve a dual utility as an active or protective component of the device. The coordination and compatibility of the manufacturing processing are necessary for the complete integration of the battery and device, which favors an all-solid-state battery (Dudney, 2013).

It would be ideal if the battery and the device were also functionally integrated. This reduces the complexity and mass of power conditioning electronics, which add complexity and mass to the device and impair overall energy efficiency. Control of the voltage range is crucial for thin film batteries, but the current for continuous charge or the time period for pulse charge can vary significantly (Dudney, 2013).

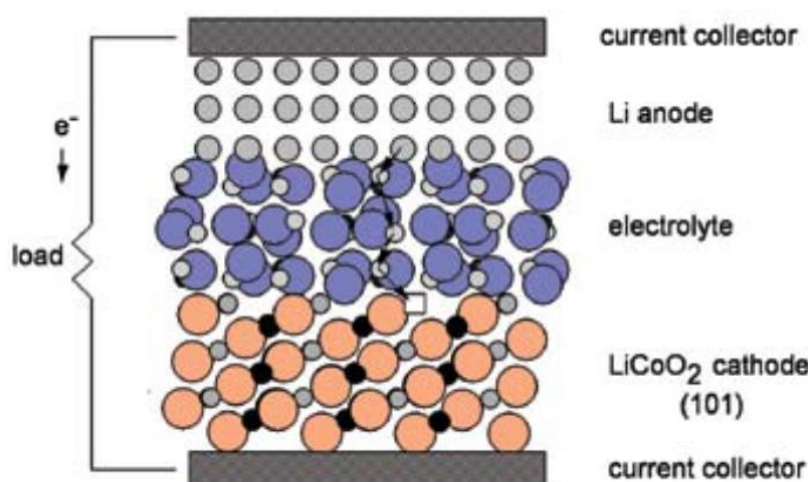


Figure 2.7 Thin film battery schematic illustration. The arrows represent the discharge reaction, in which a Li ion diffuses from the lithium metal anode to fill a space in an intercalation compound that acts as the cathode. The compensating electron travels through the device (Dudney, 2013).

Although more resilient than liquid electrolyte batteries, voltage excursions may result in extended over-charge or over-discharge situations possibly causing irreversible damage to thin film batteries. Some thin film lithium-ion batteries can resist full short circuit discharge with proper electrode selection and balance. Early coordination in the device design process allows both the device and the battery to be customised for maximum efficiency and voltage control (Dudney, 2013).

The need for a big planar battery surface to supply the device's needed energy or power may be uncomfortable or perhaps impractical for many small gadgets. A commercially viable technique for reducing the footprint involves stacking numerous units and another option is to use greater surface area substrates, such as fibres and sheets with shallow machined ridges and dimples, to provide more active area per footprint. These technologies maintain the planar battery architecture's uniform charge and current distribution. For millimetre-scale micro battery packages, efficient parallel connecting of many small cells will be required. Future advancements may lead to approaches for directly stacking batteries via vapor deposition, eliminating the bulk and mass associated with several support layers (Dudney, 2013).

In the last five years, research on thin film batteries has resulted in hundreds of articles. RFID (radio-frequency identification) tags, wireless sensors, medical devices, memory backup power, batteries for severe high and low temperatures, and energy storage for solar cells and other harvesting devices are all applications for thin film batteries. Current development initiatives are addressing manufacturing problems, particularly cost reduction. Excellent film deposition speeds, lower processing temperatures, and high yields will result from advanced processing. Exploration for new thin film materials, particularly those capable of serving as thick anode and cathode films, will increase energy and power densities. Furthermore, research into materials for optimal packing and electrical connections for multi-cell battery assembly will be vital to enabling a wide range of thin film battery applications (Dudney, 2013).

An all-solid-state thin-film lithium battery (TFB) is a thin battery made up of a positive and negative thin-film electrode and a solid-state electrolyte, typically with a thickness of less than 20mm and is suitable for use in smart cards, sensors, and micro-electromechanical systems (MEMSs) (Zhou et al., 2013).

2.5 Applications in microelectronics

Lithium-ion batteries are used in a wide variety of applications. The fast growth of electronic and information technology in the directions of multifunctionality, high integration, and high power pushed the downsizing of electronic equipment. Because the flexible cell design allows

for scaling and downsizing of other applications such as sensor packages and medical micro devices, Li-ion batteries have a large potential market in microelectronics (Patil et al., 2008; Yuxing Wang et al., 2015a).

The long-term goal of micro battery research will most likely be defined by the rapid advancement of MEMS technology, which will necessitate even higher power and higher energy on a smaller scale. Lithium micro batteries, like bulk-size batteries, can be primary or secondary. Because micro batteries in most applications are difficult to service (for example, replace), rechargeability can effectively increase a battery's service life (Yuxing Wang et al., 2015b).

Lithium micro batteries are great energy storage devices for biological/medical devices (pacemaker, hearing aid, defibrillator, in vivo imaging, and so on) as well as self-powered microelectronics (miniature transmitters, sensors, actuators, etc.) (Patil et al., 2008). Micro transmitter operation conditions need high-capacity energy storage devices capable of delivering high current pulses when needed (Yuxing Wang et al., 2015b).

Unfortunately, due to a lack of commercial cells in smaller sizes, commercial coin cells are still routinely used in these applications, so the reduction in size and improvement in capability of microsystems are currently limited by the size, capacity, and power of their on-board power supplies (Yuxing Wang et al., 2015b).

The 3D printing technology is gaining popularity, especially since printers became commercially available in recent years. When compared to other processes such as deposition and lithographic masking/etching, 3D printing produces 3D solid objects of any desired shape, making it a low-cost and versatile tool for producing 3D micro batteries (Yuxing Wang et al., 2015b).

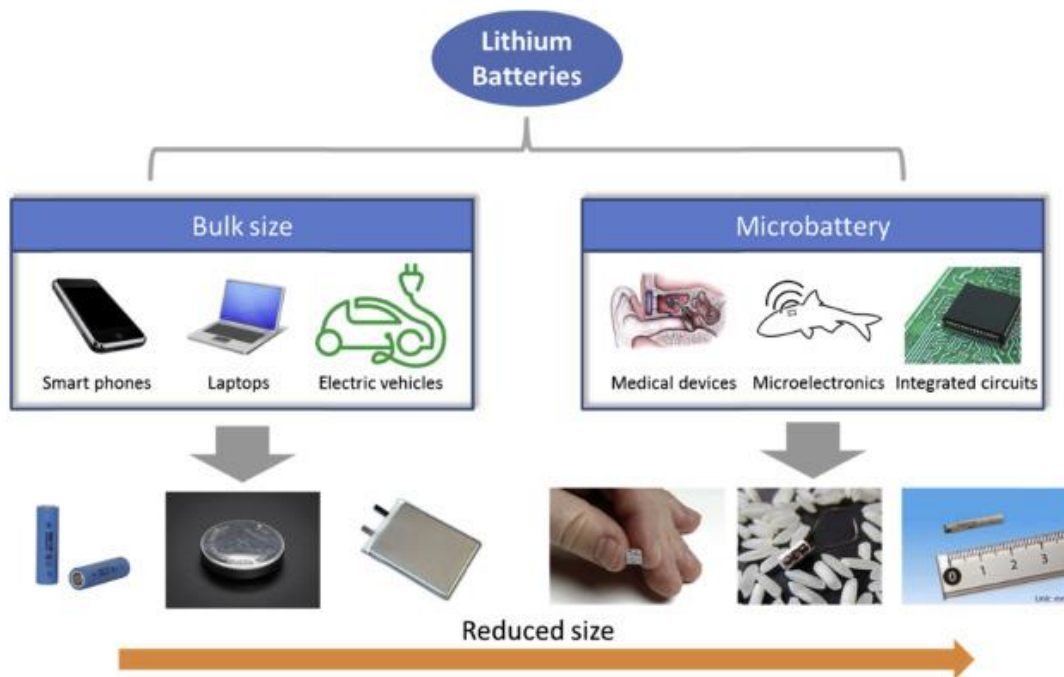


Figure 2.8 Examples of lithium battery applications and the form of cells used (Yuxing Wang et al., 2015b).

3 MATERIALS AND METHODS

3.1 Introduction

The NMC material, as aforementioned, represents one of the most used and promising cathode materials for LIBs and thus, is the material of interest. However, in terms of deposition process, it is important to firstly study and optimize the deposition of a traditional cathode, thus evolving to the final NMC thin film. In this regard, the main goal of the present work was to firstly develop LiCoO_2 coatings. In addition, diamond-like-carbon (DLC) coating was also deposited, as an anode, in order to be able to electrochemically test the battery system. The objective of this approach was to compare the potential of both coatings on a similar environment of a battery.

The films were characterized by several techniques, namely: Scanning Electron Microscope (SEM), Energy Dispersive Spectroscopy (EDS), X-Ray Diffraction (XRD), Atomic Force Microscopy (AFM), Electrochemical Impedance Spectroscopy (EIS) and Polarization Potentiodynamic (PP).

The parameters and methods used for all the experiments are going to be detailed later in this chapter.

3.2 Sputtering deposition

PVD methods are often used to deposit films with thicknesses ranging from a few nanometres to thousands of nanometres; however, they can also be used to create multilayer coatings, graded composition, and freestanding structure (Kelly & Arnell, 2000; Mattox, 2007).

Among the PVD techniques, magnetron sputtering has a big influence on applications including hard, wear-resistant coatings, low friction coatings, corrosion-resistant coatings, ornamental coatings, and coatings with particular optical or electrical properties (Kelly & Arnell, 2000), since the magnetron sputtering process allows higher deposition rates at the substrate and lower operation pressures and voltages in the discharge in relation to the basic sputtering process (Kelly & Arnell, 2000).

In the particular case of sputtering, there are different types of sputtering configurations: Cold Cathode Direct Current (dc) Diode (Non-magnetron) Sputtering, AC (including Mid-frequency) Sputtering, Radio Frequency (rf) Sputtering, Direct Current (dc) Magnetron Sputtering, Pulsed Power Magnetron Sputtering, Dual (Redundant) “Anode” Sputtering and Ion and Plasma Beam Sputtering (Mattox, 2007).

The sputtering process involves creating an electric field in a vacuum chamber between two electrodes. An inert gas is introduced into the chamber, and, because of the electric field, it becomes positively ionized and thus, colliding with the cathode of the discharge, which is the negative pole of the electric field. Atoms and molecules are ejected from the target surface toward the substrates due to the of Ar^+ ion collisions with the target material inside the cathode (Kelly & Arnell, 2000) (Figure 3.1). Argon is typically used for inert gas sputtering since it is an affordable inert gas (Calderon Velasco et al., 2016).

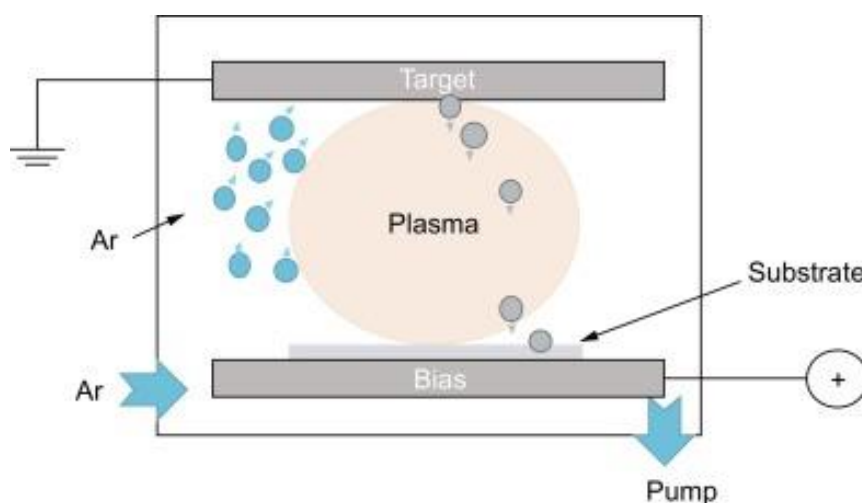


Figure 3.1 Plasma process inside the chamber (*Chapter 11 - Bioactive Surface Coatings for Enhancing Osseointegration of Dental Implants*, 2019).

In this project it is intended to develop an active and multifunctional LiCoO_2 thin film cathode and a DLC thin film anode.

The system used and available in Instituto Pedro Nunes (IPN) to deposit the thin films was a Direct Current Magnetron Sputtering (DC-MS) machine is represented in Figure 3.2. The Figure 3.3 is the screen of the computer/control station and represents a scheme of the system in Figure 3.2.

This system is composed by a cylindrical deposition chamber with 38cm internal diameter and 50 cm height, contain two planar targets with magnetron system connected to a DC-pulsed power supply (*Advanced Energy Pinnacle Plus*), three power sources, three flowmeters to inject gases and their controller, two pressure sensors (*Edwards wide range gauge WRG-S* and *Pfiffer barocel capacitance manometer TPG 362*) and an entry of water at 19.5°C to cooled down the substrate.

The system also had a substrate motor that can put the substrate holder in rotation or in static mode. This substrate holder is approximately at a distance of 130 mm from the target and rotates at a maximum speed of 20 rpm during deposition.

The chamber, where the depositions took place, is connected to a primary rotary pump (*Pfeiffer Vacuum DUO 20 M*, pumping speed 20 m³/h) and a secondary diffusion pump (*BOC Edwards Diffstak 160/700*, pumping speed 760 l/s).

A good plasma system for PVD processing must first be a good vacuum system. Vacuum systems used in vacuum deposition processing are primarily used to reduce polluting residual gases and vapours to acceptable levels.

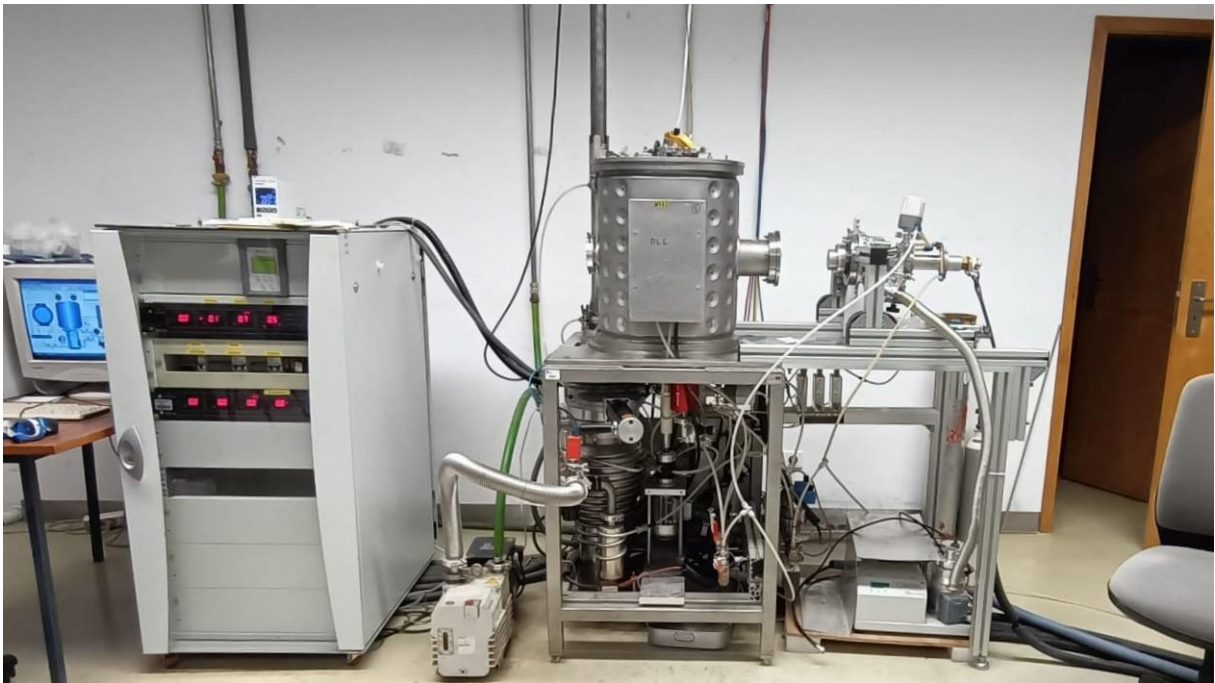


Figure 3.2 Direct Current Magnetron Sputtering system.

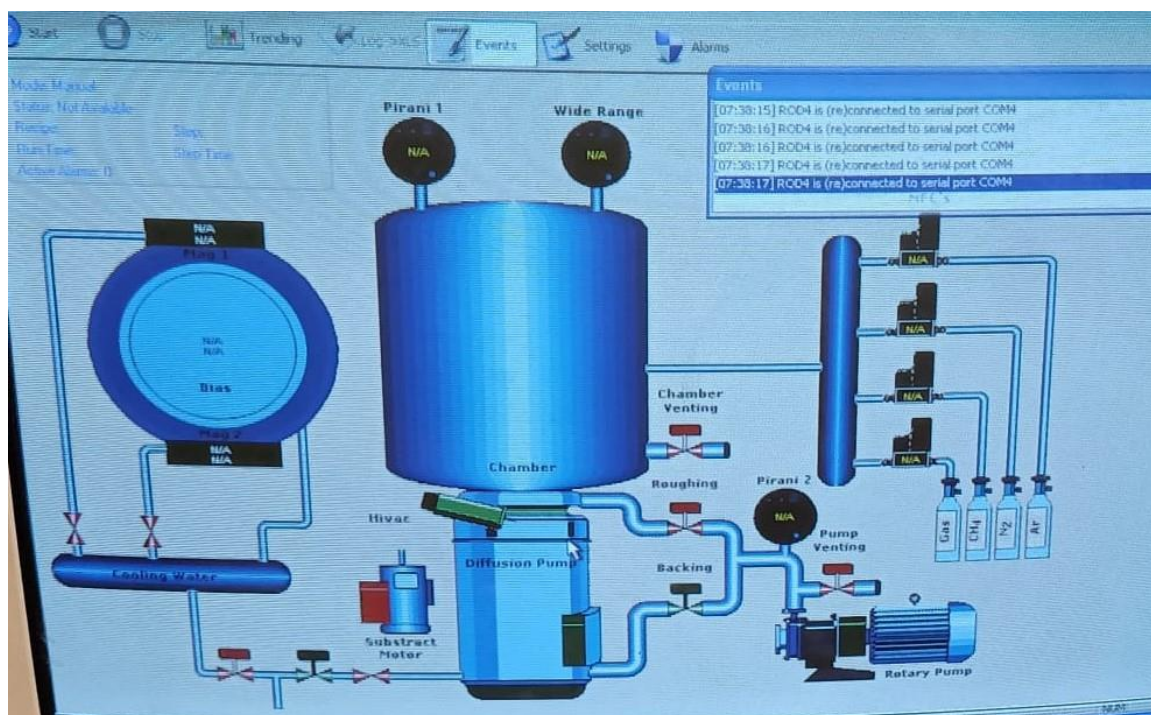


Figure 3.3 Schematic representation of de DC MS system.

3.3 Experimental details of LiCoO₂ deposition

For this experiment it was used a target of LiCoO₂ with the dimensions of 200x100x10mm³, silicon (Si) and glass were used as substrates and 15% of Argon (Ar) (correspond to 37.5sccm) was used as the neutral gas.

Before the depositions, the substrates were cleaned in an ultrasonic cleaning equipment: firstly, with acetone (C₃H₆O) and after with ethanol (C₂H₆O), ten minutes each, to remove superficial impurities, prevent contaminations, and improve the adhesion between substrate and deposited film.

The vacuum was guaranteed setting up first the primary pump that induced the primary vacuum, up to proximally 10⁻³ Pa, and after a secondary pump until 10⁻⁴ Pa as late as the morning after.

Therefore, it was necessary to clean the target surface with the deposition of this same target with maximum power possible and the initial parameters of Table 3.1.

Table 3.1 Initial parameters of the Magnetron Sputtering system of LiCoO₂ deposition.

Voltage	Intensity	Power	Time Period	Frequency
500V	0.47A	237W	2.9ns	155kHz

The depositions itself were conducted with the same conditions of Table 3.1. First, it was tried a deposition of 50 minutes and other with however no traces of the thin film were found in SEM-EDS or profilometer. Therefore, it was tried 2hours30min of deposition with a static substrate, but again no traces of the thin film were found in the profilometer. Still, a 0.01% presence of Cobalt in SEM-EDS suggesting some materials have been deposited.

In Noh et al., 2012 it was possible to obtain a thin film cathode within 20 minutes but had lack of information about the dimensions of the target and the chamber, per example.

In one last attempted, it was tried a 12 hours deposition with the substrate holder in static rotation obtaining a thin film not ideal but possible to characterize.

3.4 Experimental details of Carbon deposition

In the case of the DLC coatings, the substrates used in this deposition were silicon (10×10 mm²) and glass. Before this deposition the Si and glass substrates were also cleaned in an ultrasonic bath with acetone, ethanol, and distilled water, ten minutes each.

Following instructions of the experimental approach in the paper Carvalho et al., 2020, the depositions of DLC were performed in an 15% Ar atmosphere (37.5sccm) and with a working pressure of 3.7×10^{-3} mbar, with a 10rpm constant rotation speed of the substrate holder, during 120 min. The power, voltage and intensity of the experiment was, respectively, 600W, 700V and 0.86A.

3.5 Characterization techniques

3.5.1 Scanning electron microscopy and energy dispersive X-ray spectroscopy

Scanning electron microscopy (SEM) and energy dispersive X-ray spectroscopy (EDS) is an “advanced” surface analysis tool that allows the study of sample surfaces and chemical composition, respectively, for targeted analysis. SEM and EDS analysis are employed when it is needed a high resolution, high depth of field image, as well as, when it is necessary an elemental composition for a bulk material or a specific portion of that material. Therefore, these techniques are normally used for material surface analysis, investigation of product failures, reverse engineering, contaminant identification, solder joint analysis and more.

The technique's imaging component is SEM. The electron optics and sample interaction of the SEM determine its magnification and resolution, allowing a larger depth of focus. Usually coupled with SEM it is possible to find the EDS detector that allows to quantify the energy of photons released into the X-ray electromagnetic spectrum. With the spectrum, it is possible to identify the peak energies and determine what electron transition occurred and thus what

element it corresponds to. This data can be couple to the SEM imaging technique to form X-ray “maps” of data to overlay or present areas of high individual elemental concentrations (RTI Laboratories, 2020).

For this work, we used a SEM from Hitachi, model Su3800, with an acceleration voltage of 1 and 2 kV for the SEM imaging and 15 kV for EDS analysis.

3.5.2 X-Ray Diffraction

X-Ray diffraction (XRD) is a versatile, non-destructive analytical technique for identifying and quantifying the many crystalline forms of substances found in powdered and solid materials. Identification is accomplished by comparing an unknown sample's X-ray diffraction pattern (diffractogram) to a global database containing reference patterns for over 70 000 phases (PANalytical).

Particularly, a cathode ray tube generates X-rays, which are then filtered to produce monochromatic radiation, collimated to concentrate, and directed toward the sample. When the incident rays contact with the sample, they create constructive interference and a diffracted ray if the conditions satisfy Bragg's Law ($n\lambda=2d \sin \theta$). This law describes the relationship between the wavelength of electromagnetic radiation and the diffraction angle and lattice spacing in a crystalline sample. After that, the diffracted X-rays are detected, processed, and tallied. Due to the random orientation of the powdered material, all potential diffraction directions of the lattice should be reached by scanning the sample through a range of 2θ angles (Dutrow, 1912). In this work, X-Ray diffraction was performed by the PANalytical X'Pert PRO MPD with $\text{CuK}\alpha$ radiation (40kV and 35mA) and $\theta = 2^\circ$.

3.5.3 Atomic force microscopy

Atomic force microscopy (AFM) is a type of scanning probe microscopy that physically contacts and scans a sample's surface in order to produce images with a resolution of just a few nanometers. To create a 3D image of the surface topography, it measures the force of interaction between the probe and the sample (NanoAndMore, 2022) (Figure 3.4).

AFM have two basic modes to image surface topography: Static or Contact Mode and Dynamic Mode. Depending on the interaction forces between the AFM tip and the surface, Dynamic Mode is subdivided into Tapping or Intermittent Contact and Non-Contact Mode (NanoAndMore, 2022).

In Contact Mode the AFM probe tip maintain constant contact with the sample surface and the forces between them are repulsive, while Non-Contact Mode the AFM probe tip is kept

some nanometers away from the surface and have attractive interaction forces (NanoAndMore, 2022).

In Tapping Mode, the predominant forces between the AFM tip and surface are repulsive and the AFM probe tip oscillate by a piezoelectric actuator near its fundamental resonance frequency and slightly touches the surface at the lower end of the AFM cantilever oscillation (NanoAndMore, 2022).

In this thesis AFM of the LiCoO_2 film in the silicon substrate was conducted on a Veeco DiInnova in tapping and oscillating mode with a 10nm tip. The thickness of the sample was obtained using the open-source software Gwyddion 260.

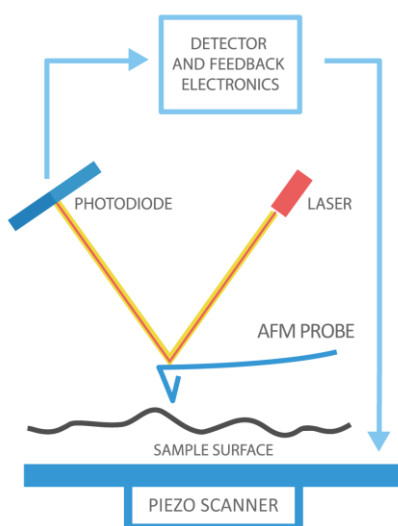


Figure 3.4 AFM schematic.

3.5.4 Potentiodynamic polarization and Electrochemical impedance spectroscopy

Potentiodynamic polarization (PP) is a technique that applies a current through the electrolyte to change the electrode's potential at a chosen rate (Corrosionpedia, 2019).

Electrochemical impedance spectroscopy (EIS) is an electrochemical technique where the impedance or resistance of a material to an electrical current as a function of frequency is measured by applying a small ac voltage signal. EIS provides information on the electrochemical kinetics, corrosion behaviour, and charge transfer resistance of the examined

material. The results are then used to create a Nyquist plot, which is a graphical representation of the impedance data (Magar et al., 2021).

In this work, the electrochemical tests were carried by PP and EIS.

PP and EIS was carried out in a Gamry 600 potentiostat. Each sample were performed in a Faraday cage to isolate the experiments from external interferences. It was used a three-electrode setup where the working electrode was the sample, the reference electrode was a calomel electrode saturated in KCl and the counter electrode was a pure platinum plate. EIS and PP were conducted on both films, three analyses for each, in an 1M NaOH alkaline solution ($\text{pH} > 7$), at room temperature, windless and in static mode.

The parameters used in the potentiodynamic scans are displayed in Table 3.2. The sweep was always versus open circuit potential. Data were collected after one hour, to ensure that the sample had stabilised.

Table 3.2 Potentiodynamic scans parameters.

Initial E	Final E	Scan Rate	Sample Period	Sample Area	Open Circuit
-0.5 V	0.5 V	1 mV/s	1 s	0.28 cm ²	-0.203257

4 RESULTS

4.1 Introduction

This dissertation is divided in two main stages: (1) production of the materials; and (2) its fundamental and electrochemical characterization.

Particularly, each material deposited was characterized by using Electron Microscopy coupled Energy Dispersive Spectroscopy (SEM-EDS), X-Ray Diffraction (XRD), Atomic Force Microscopy (AFM), Potentiodynamic polarization (PP) and Electrochemical Impedance Spectroscopy (EIS), depending on the various results.

4.2 Chemical composition and surface characterization

Two coatings were deposited: a LiCoO_2 coating to represent a cathode and a DLC coating to represent an anode. To get the morphology of the LiCoO_2 film on the silicon substrate was used cross section SEM, without success. This approach could not identify the coating morphology since it was less than 50nm thin, underneath the system detection limit, as later observed in the profilometer. So, it was recommended to use AFM since the resulting LiCoO_2 film was too thin to get a thickness and topography image by SEM.

In Figure 4.1 and in Figure 4.2, it is possible to observe that DLC and LiCoO_2 films, have, 260.5 nm and 40 nm as thicknesses respectively.

As seen in Figure 4.1 and Figure 4.3 the DLC film has a columnar morphology, with some porosity. The Figure 4.4 is not very clear, but the AFM image, displayed in Figure 4.5, revealed an irregular surface where the dominant colour in the image shows the most common topography of the LiCoO_2 film, is approximately 40 nm.

Since the DLC film is made essentially of Carbon and the typical chemical contaminations founded in thin films deposited by MS is carbon as well, the chemical characterization of this film was not performed.

The chemical composition of the LiCoO_2 coating obtained by EDS is presented in Table 4.1. In order to statically validate the results three measurements were performed. The glass substrate's EDS examination of the LiCoO_2 showed several contaminations, including Sn, and too many glass-specific elements, reason why therefore, EDS analysis was performed over silicon substrates. However, as shown in Table 4.1, the Si substrate examination also revealed contaminants like Ti and Cr that should not be present in the film composition.

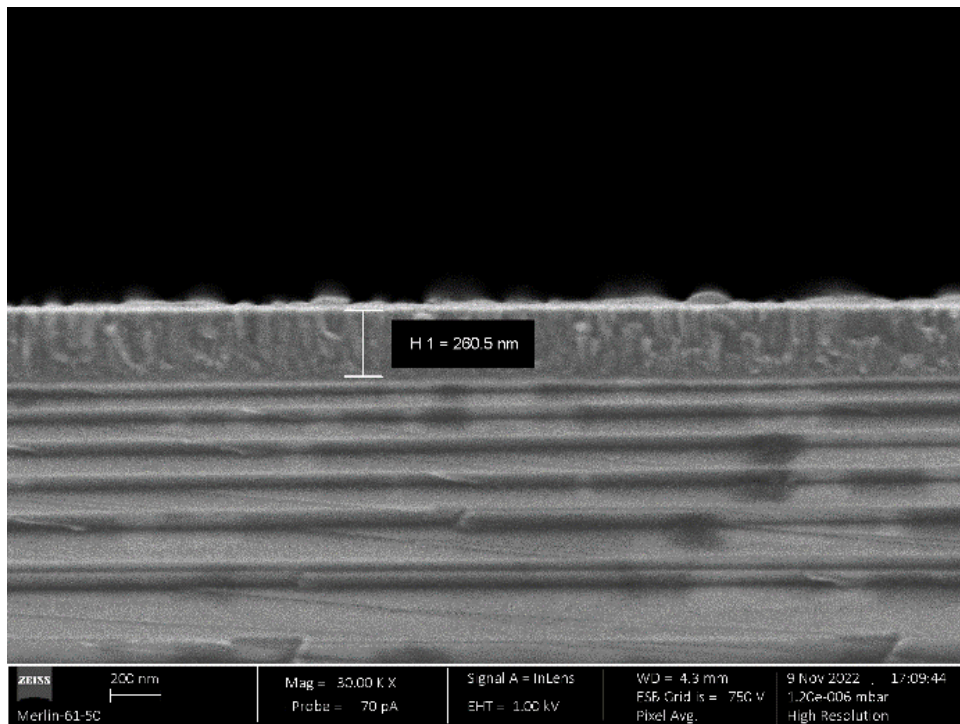


Figure 4.1 Cross section by SEM of DLC film.

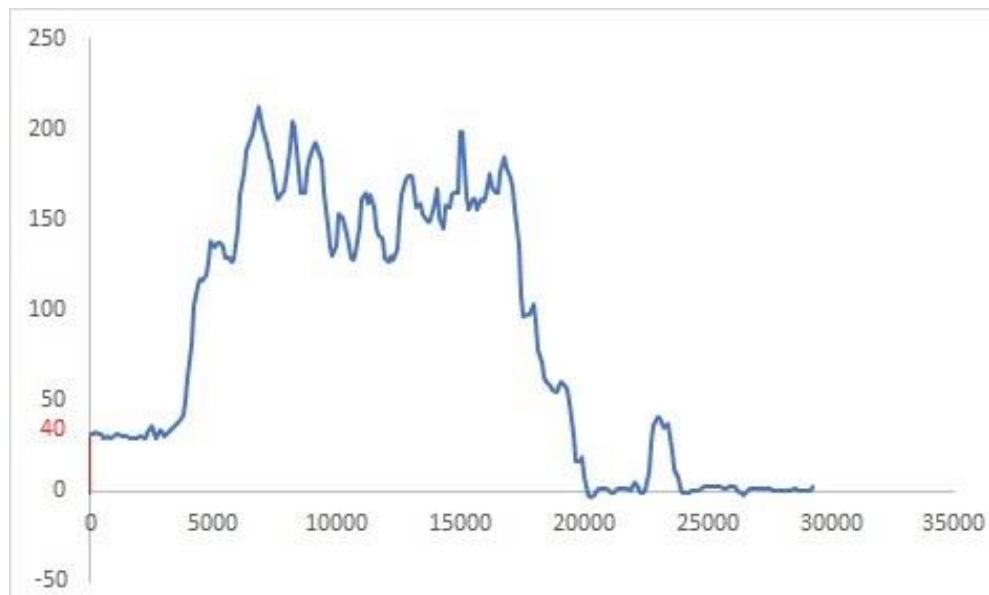


Figure 4.2 Thickness of LiCoO₂ film by AFM.

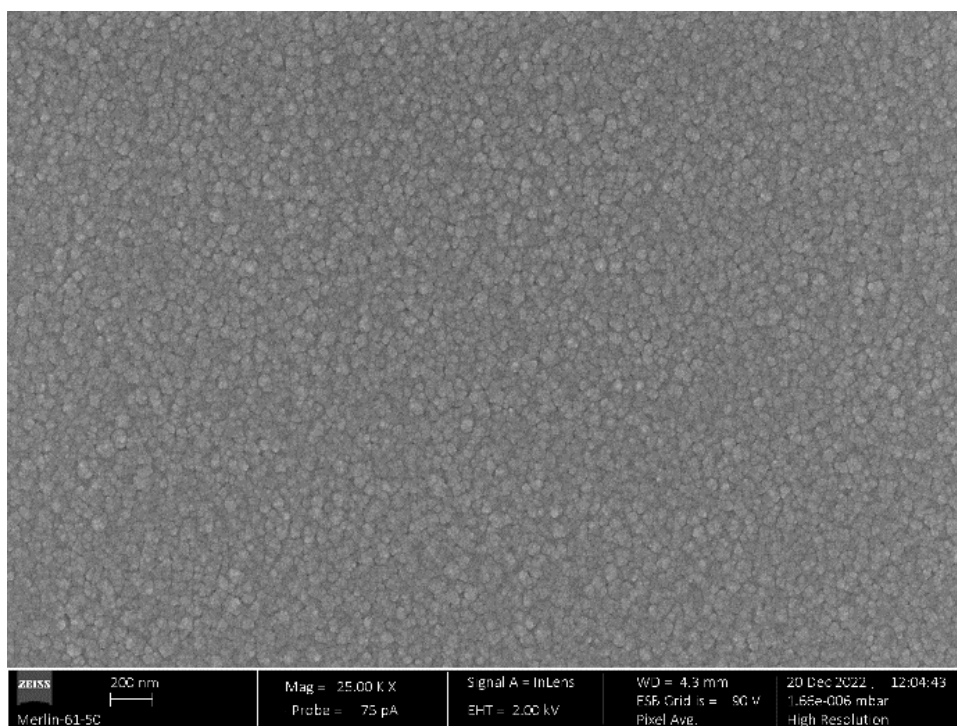


Figure 4.3 Surface of DLC film by SEM.

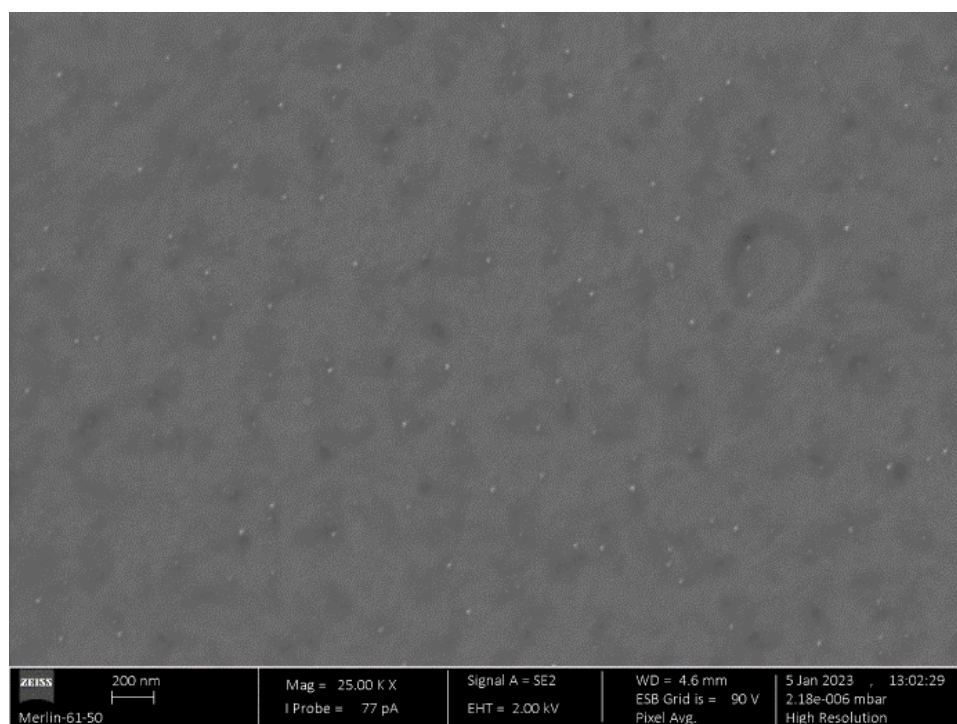


Figure 4.4 Surface of LiCoO₂ film by SEM.

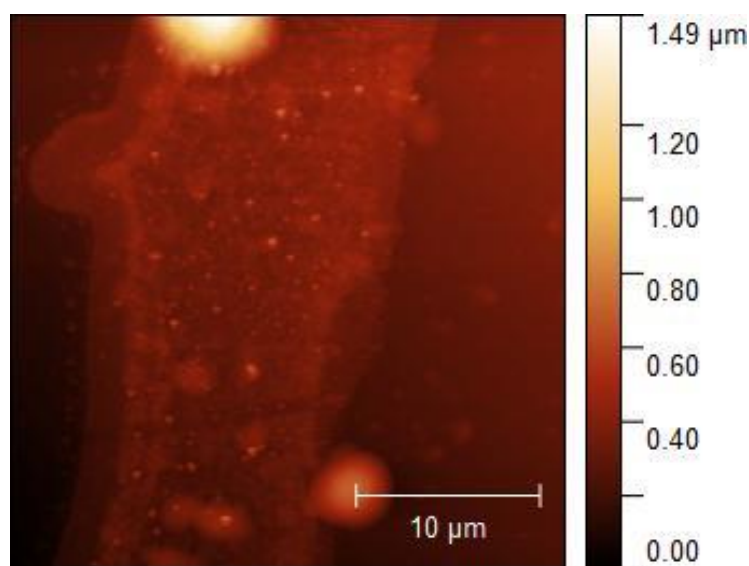


Figure 4.5 AFM of LiCoO₂ film.

In order to try to mitigate these materials contamination from the LiCoO₂ thin film on glass, the Cr target was removed, and the magnetron was both covered with a metal plate, and a shutter. Yet, the Cr contaminations remained with a similar percentage in the glass substrate. Soon, the target of LiCoO₂ will be examined to determine if there are any manufacturing flaws.

Table 4.1 Chemical composition of LiCoO₂ coating.

	Spectrum Label	O (at.%)	Ar (at %)	Ti (at %)	Cr (at %)	Co (at %)	Total (at %)
Deposition in silicon substrate	LiCoO ₂ 21.12 Sp 1	44	3	1	5	47	100
	LiCoO ₂ 21.12 Sp 2	44	3	1	6	46	100
	LiCoO ₂ 21.12 Sp 3	44	3	1	6	47	100
	Average values	44	3	1	6	47	100
	Standard deviation	0.09	0.15	0.13	0.34	0.16	0

4.3 Structural characterisation

The X-Ray diffractograms of the LiCoO₂ and DLC coatings are presented in Figure 4.6 and Figure 4.7, respectively. The results of the XRD measurements shows that both coatings have an amorphous structure.

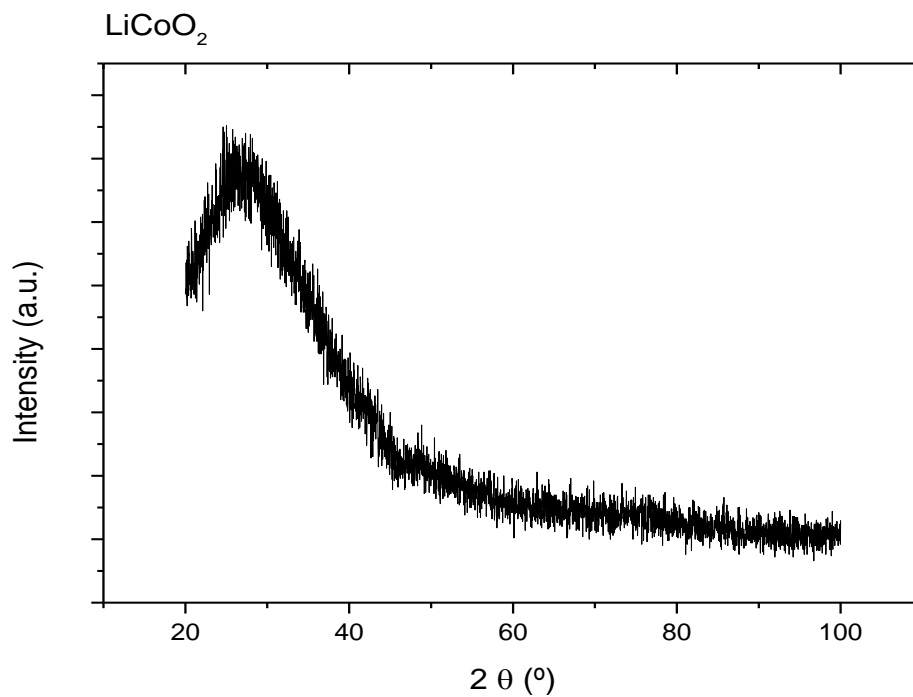


Figure 4.6 X-Ray diffractogram of LiCoO₂ coating.

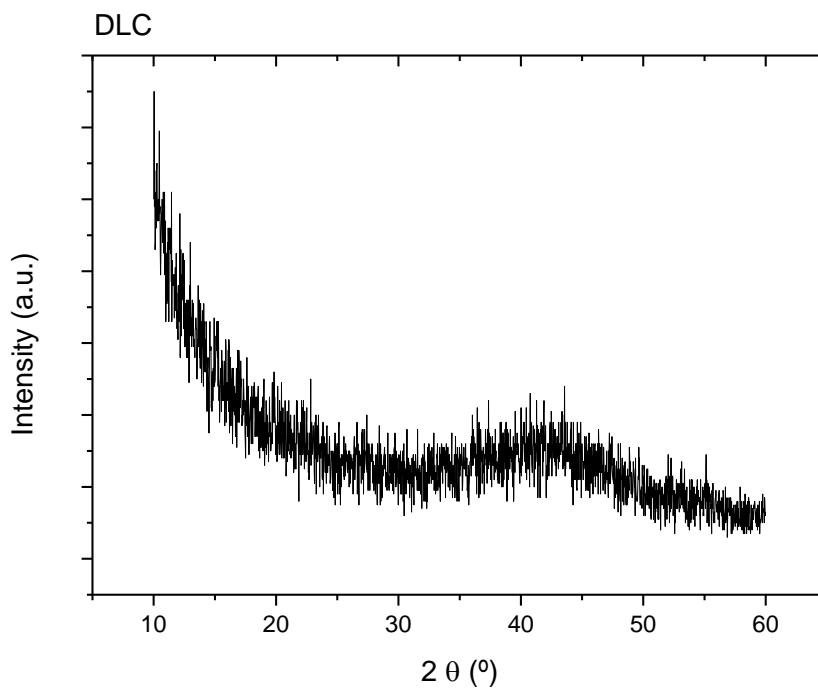


Figure 4.7 X-Ray diffractogram of DLC coating.

4.4 Electrochemical performance

Ideally, to evaluate the electrochemical performance, charge-discharge tests would be performed. However, those tests were not available at the laboratory. In this regard, firstly PPs were performed to identify the potential between the anodic and cathodic regions of each material. Thus, EIS was measured in the region where LiCoO_2 behaves like a cathode, and DLC behaves like an anode. Afterwards, the EIS tests were performed by exchanging the behaviour of the studied films (LiCoO_2 as the anode and DLC as the cathode). The EIS measurement was performed to simulate charge-discharge processes of a battery and to establish the electrochemical behaviour of the deposited coatings in the working regime.

The corrosion rate commonly is calculated by using ASTM-G102, although the equivalent weight may affect the results. Since the composition of the samples, is not 100% known, it was not possible to precisely determine the corrosion rate. Even then, we can evaluate qualitatively the corrosion resistance. With the individual E_{corr} values, we can establish a galvanic series for a corrosive environment, which is, a scale of "nobility" or resistance. As can be observed in the Figure 4.8, since the E_{corr} of the anodic polarization curve of DLC is higher than the LiCoO_2 we can say that DLC film is nobler than the LiCoO_2 film. However, both are resistant to corrosion.

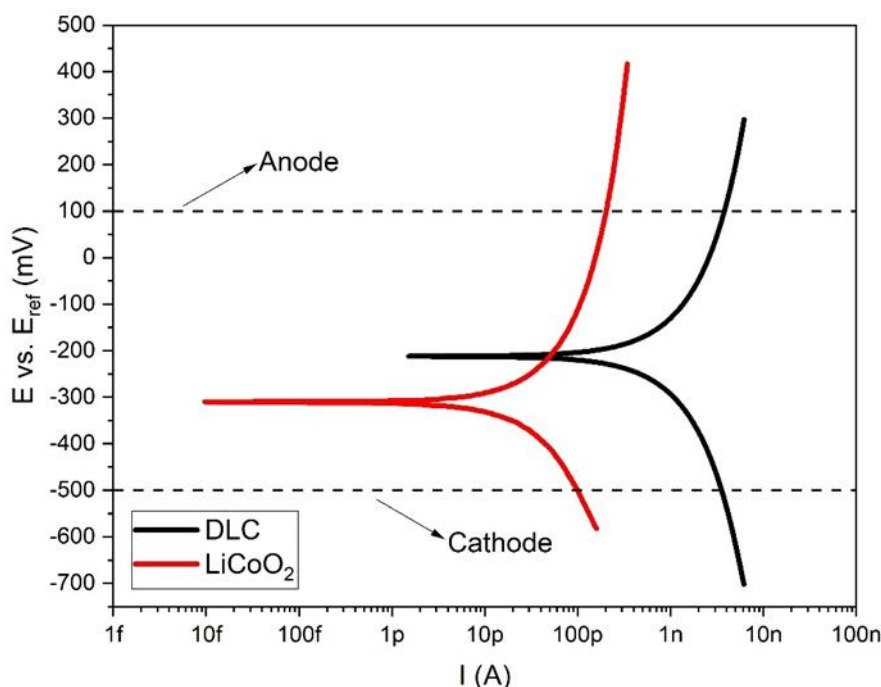


Figure 4.8 Polarization curves of DLC and LiCoO_2 coatings.

Table 4.2 provides fitting parameters for all coatings and the uncoated substrate, including anodic (β_a) and cathodic (β_c) slopes, corrosion potential (E_{corr}), corrosion current density (J_{corr}) and corrosion current density (I_{corr}).

Table 4.2 Fit parameters of polarization potentiodynamic curves from samples in 1M of NaOH solution.

	β_a (mV/decade)	\pm	β_c (mV/decade)	\pm	I_{corr} (nA)	\pm	J_{corr} (A/cm ²)	\pm	E_{corr} (mV)	\pm
DLC	1026.75	233.25	1008.00	230.00	2.78	0.70	9.93E-09	2.50E-09	-188.00	24.00
LiCoO ₂	3129.00	1863.00	1179.50	53.50	0.933	0.80	3.33E-09	2.85E-09	-246.00	65.00

The Pourbaix diagram show the stability of a metal as a function of pH and potential. The Pourbaix diagrams of Li, Co and C shown in Figure 4.9, Figure 4.10, and Figure 4.11 show the most probable compound formation of the films in 1M of NaOH solution.

Considering the 1M NaOH solution it was assumed a standard pH between 10 and 12. Since the E_{corr} of DLC and LiCoO₂, is -188 and -246mV the Pourbaix diagrams show the types of corrosion products that are likely to form in this environment: Li(+a), Co₃O₄ and NaCo₃(-a). The formation of this compounds allows the mobility of Li-ion, suitable for the intended battery charge and discharge processes, where lithium ions move from the positive electrode through the electrolyte to the negative electrode and deposit between carbon layers and in reverse in the discharge process. Thus, suggesting that the combination of LiCoO₂ and DLC thin films is appropriate for a thin film battery system.

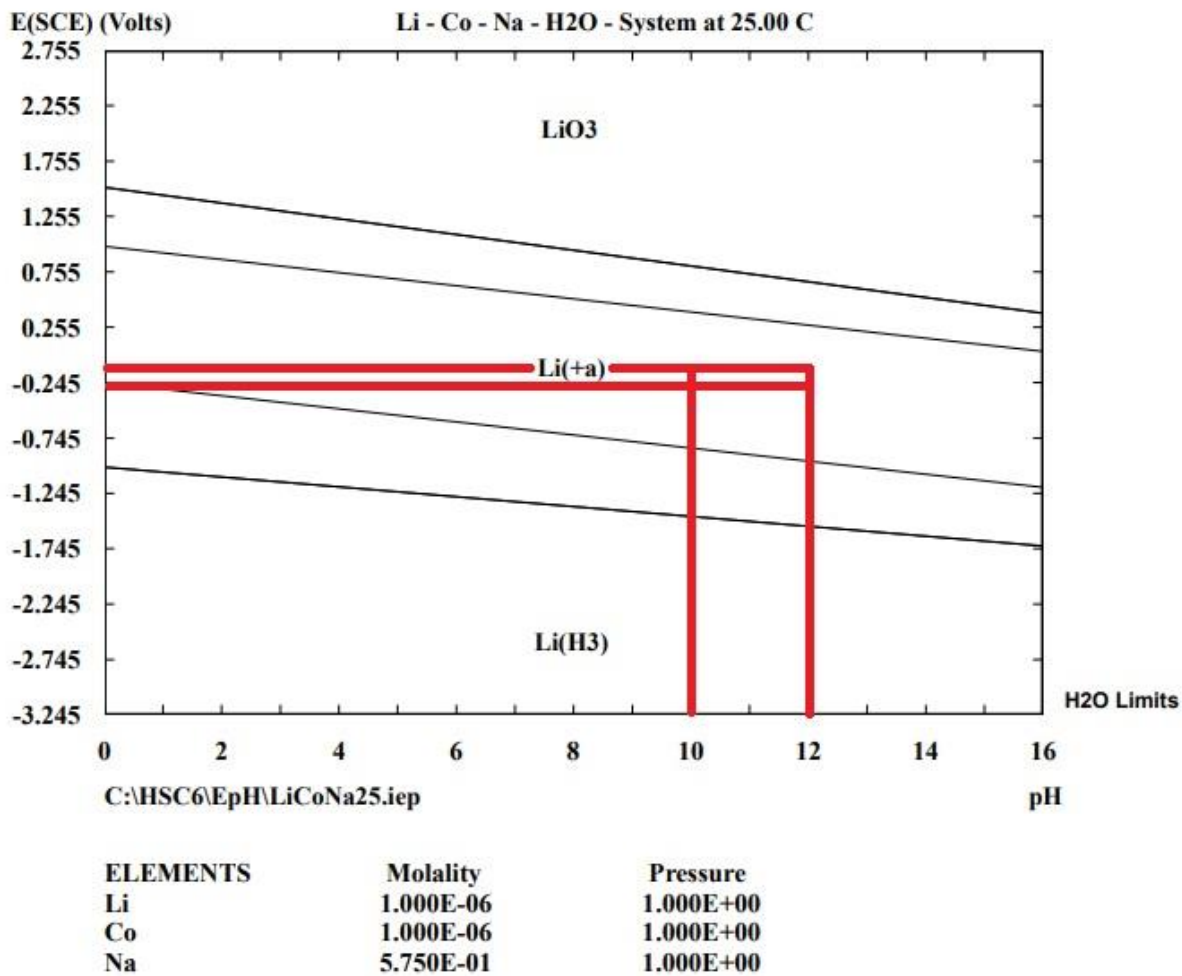


Figure 4.9 Pourbaix diagram of Li.

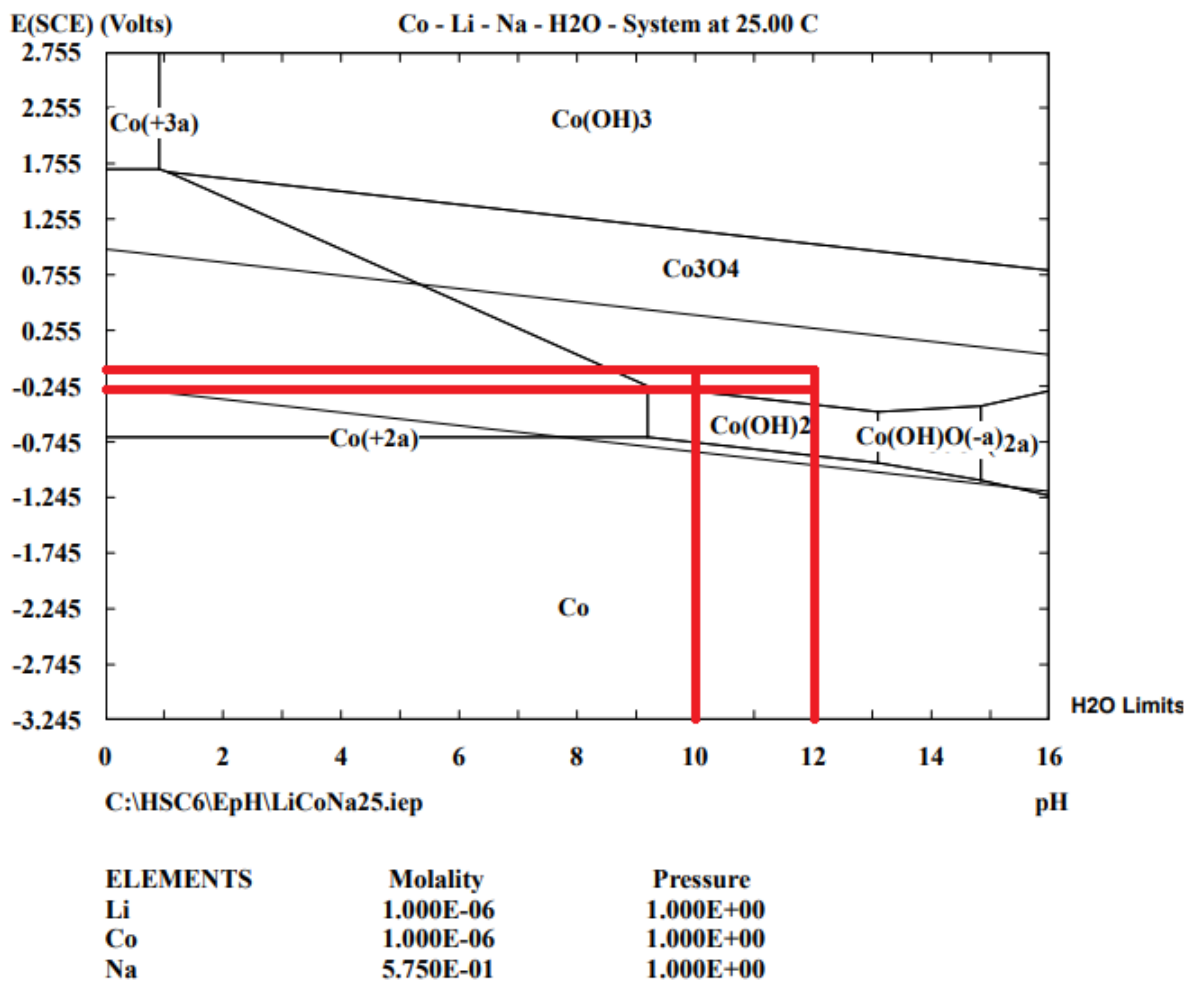


Figure 4.10 Pourbaix diagram of Co.

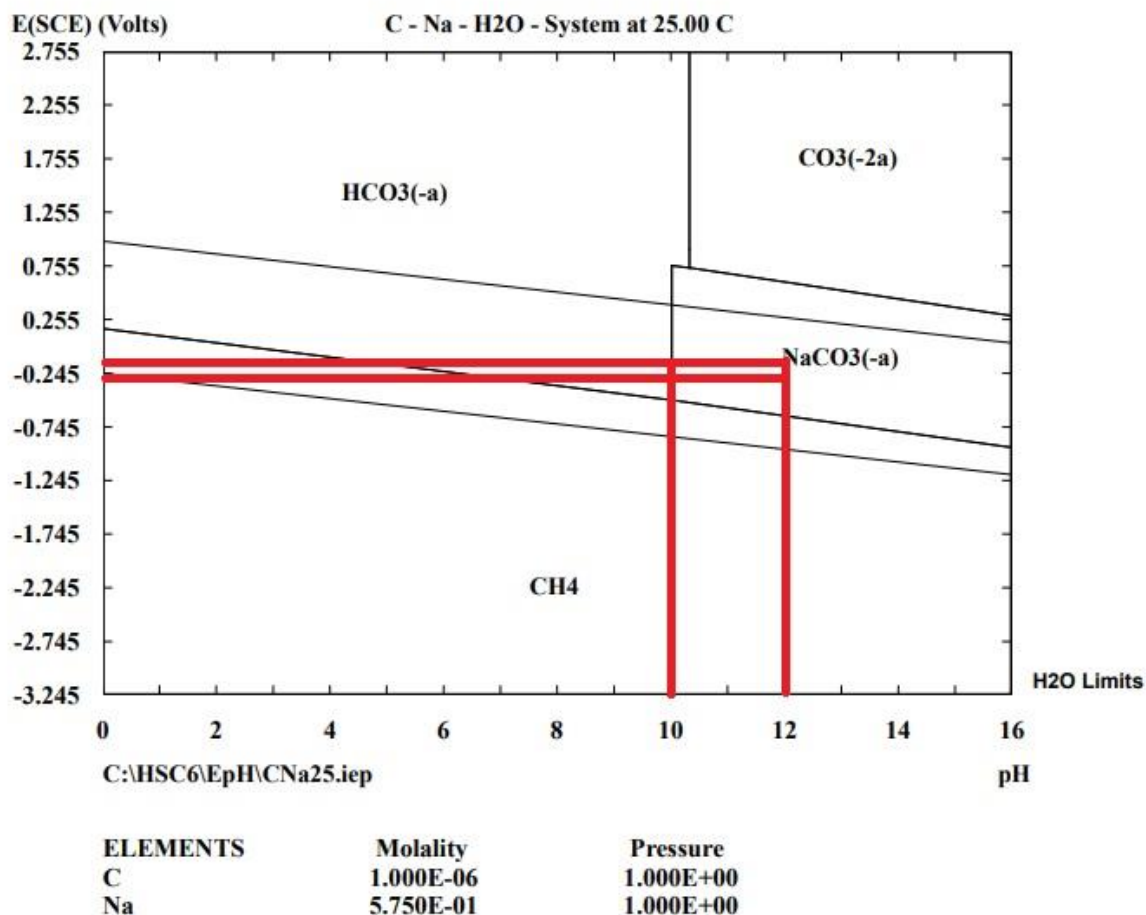


Figure 4.11 Pourbaix diagram of C.

To study the electrochemical response of the obtained films and possible components present the EIS was conducted at open circuit potential (OCP), obtaining the result presented in bode and phase angle in Figures 4.12, 4.13, 4.14 and 4.15. The bode and phase angle plots, demonstrated the presence of one-time constants.

The Nyquist plots in Figures 4.16 and 4.17 verified that the presence of one-time constant in the two thin films, i.e., along the time the thin films corrode at the same rate. One-time constant is the duration necessary to fill the capacitor with 63% of its full capacity or, in other interpretation, to drop 37% of the initial value of the current. Usually, higher time constants indicate slower corrosion rates and greater resistance to corrosion (Sorting Hat Technologies Pvt Ltd, 2023).

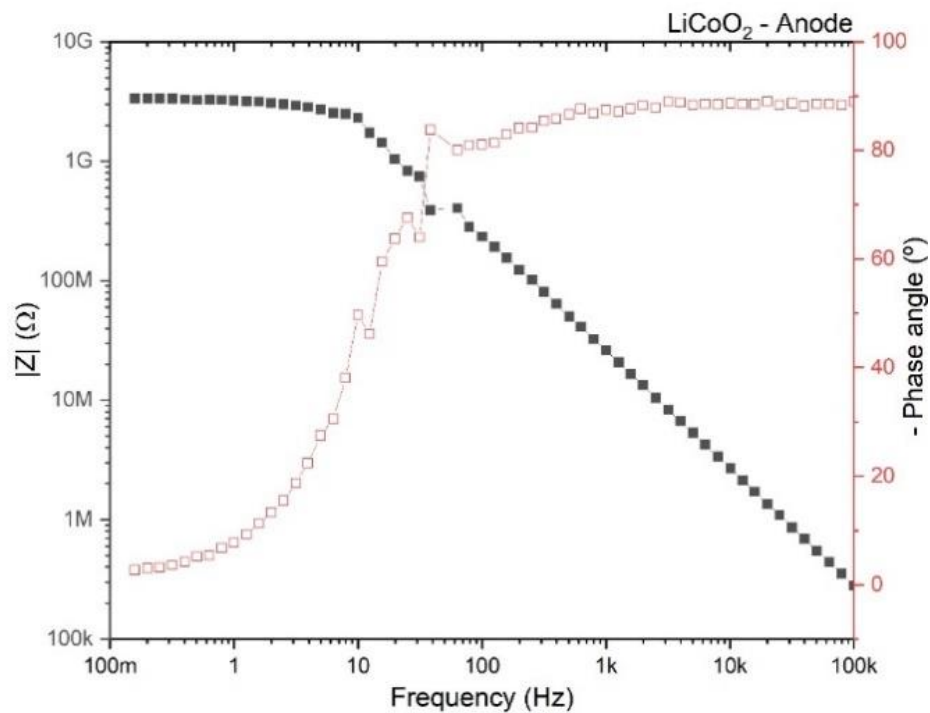


Figure 4.12 Bode and phase angle plots of LiCoO₂ as an anode.

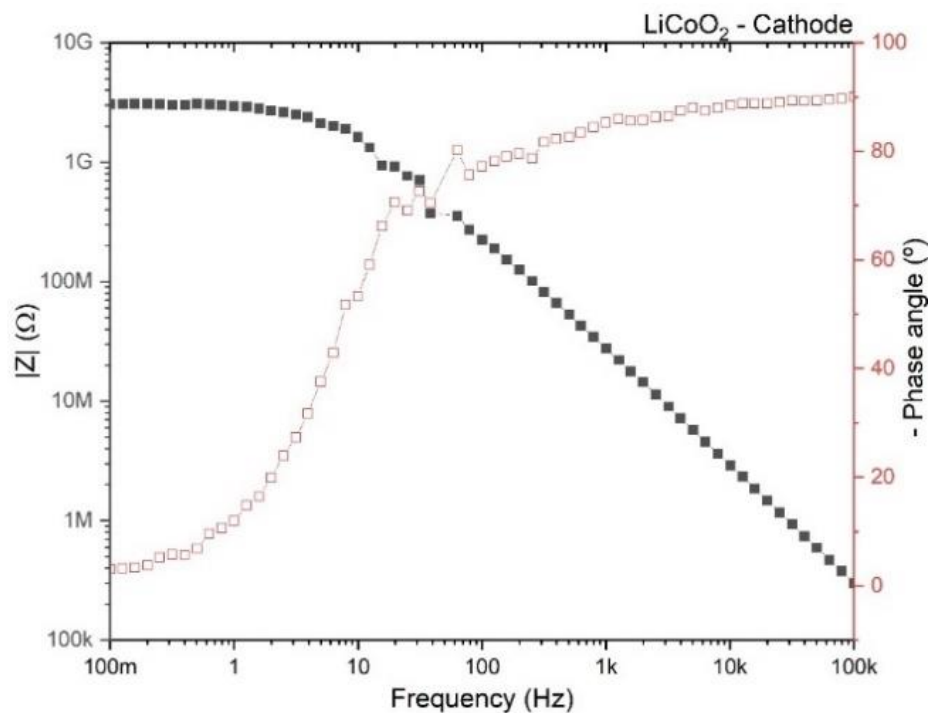


Figure 4.13 Bode and phase angle plots of LiCoO₂ as a cathode.

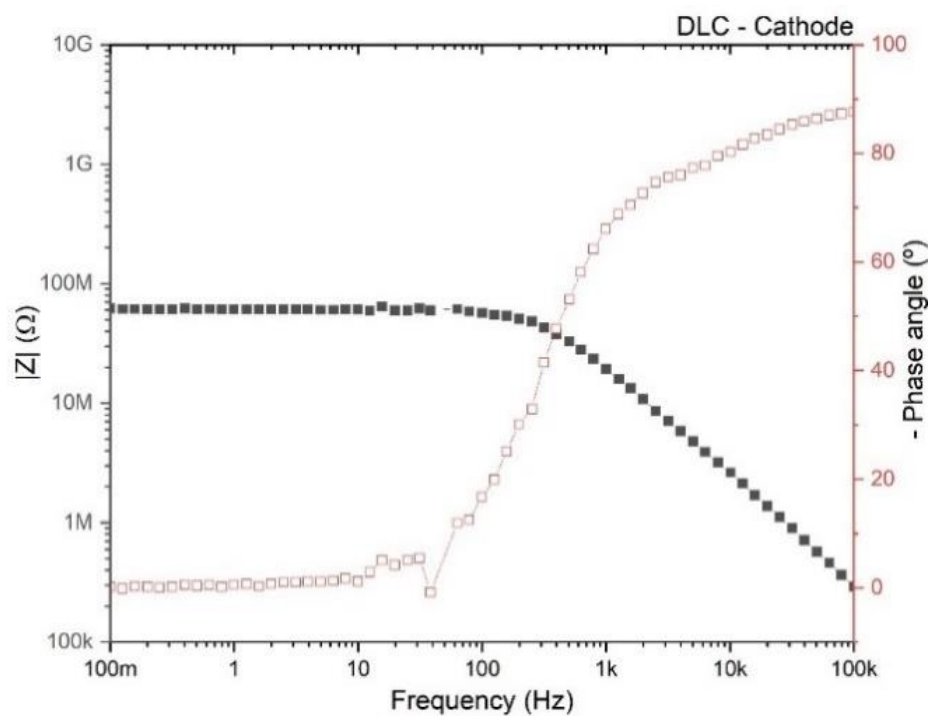


Figure 4.14 Bode and phase angle plots of DLC as a cathode.

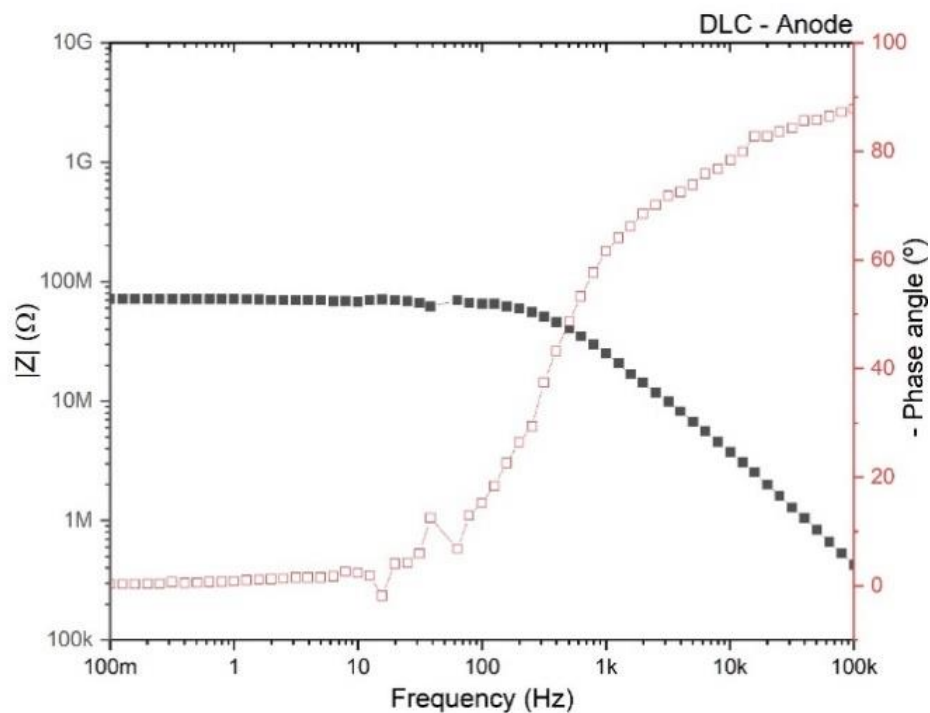


Figure 4.15 Bode and phase angle plots of DLC as an anode.

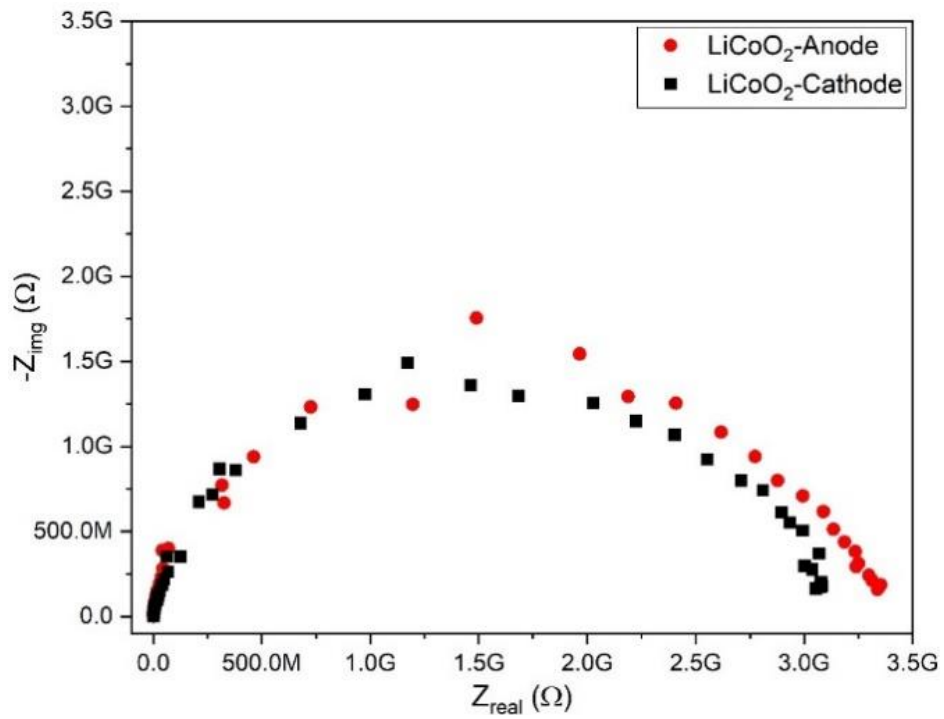


Figure 4.16 Nyquist plots of LiCoO₂.

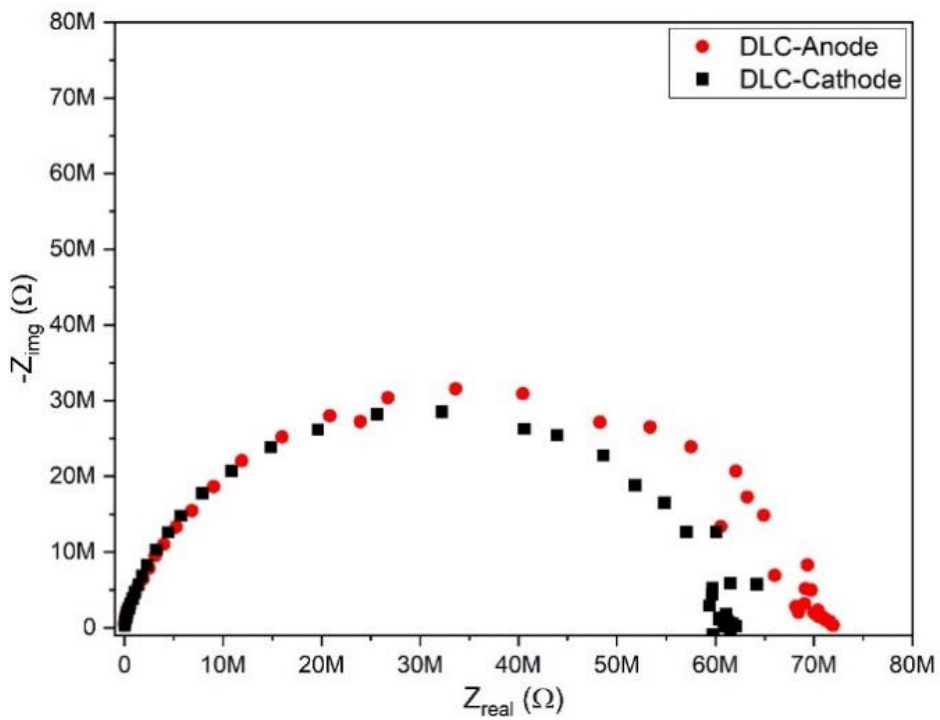


Figure 4.17 Nyquist plots of DLC.

The equivalent electric circuits (EEC) used to fit the EIS measurements (Table 4.3 and 4.4) are represented in Figure 4.18, Figure 4.19 and Figure 4.20. These circuits can be constituted by R_{liq} , the resistance of the electrolyte, R_{pore} , the resistance of the pore, R_{film} , the resistance of the coatings, C_{pore} , the capacitance of the pores, C_{film} , the capacitance of the film, W , the diffusion, CPE_{film} , the constant phase element (CPE) of the coating and α , the exponent in the CPE. The Goodness of fit correspond to the deviation of the adjustment to reality. Using the different parameters, it is possible to verify different electric responses.

In all the EEC, R_{liq} and R_{pore} , represents the resistance of the electrolyte solution around the films and the resistance of the pores within the coating's materials, respectively, while in the EEC in Figure 4.18, R_{film} represents the resistance of the coatings materials themselves. These resistances are necessary to include in the EEC to model the behaviour of the coating's materials.

In the EEC in Figure 4.18, C_{pore} represents the capacitance of the pores within the DLC film and C_{film} represents the capacitance of the DLC film. C_{pore} and C_{film} are necessary to include in the equivalent electrical circuit of DLC coating to model the behaviour of the film in relation to the pores and to model the behaviour of the film as a dielectric material, the film capacity to store electrical charge in an electric field, respectively.

On its turn, the $LiCoO_2$ film does not exhibit a pure capacitive or resistive behaviour, so it cannot be represented only by capacitance or resistance components. Therefore, it's necessary to include in its EEC, shown in Figure 4.19 and in Figure 4.20, the constant phase element to model its behaviour of the $LiCoO_2$ film.

When $LiCoO_2$ film behaves like an anode typically ions are insert and removed of the film by diffusion process and by including the diffusion element on the equivalent electric circuit it's possible to model the diffusion process in the $LiCoO_2$ coating. However, the $LiCoO_2$ coating is very thin and thus, the diffusion processes when it behaves like a cathode could not be determined.

Table 4.3 Fit parameters of EIS of DLC according to the equivalent electric circuit.

	R_{liq} (Ω)		R_{pore} (Ω)		C_{pore} (F)		R_{film} (Ω)		C_{film} (F)		Goodness of Fit
DLC-0h- Anode	4.96E +04	1.88E +03	5.57E +07	2.62E +06	4.61E -12	2.44E -14	1.49E +07	3.00E +06	8.20E -10	4.56E -10	3.47E-02
DLC-0h- Cathode	9.80E +03	3.17E +02	1.46E +07	3.83E +05	5.59E -12	2.37E -14	4.53E +07	2.78E +05	3.82E -12	2.88E -13	1.52E-02

Table 4.4 Fit parameters of EIS of LiCoO₂ according to the equivalent electric circuit.

	R _{liq} (Ω)		W (S*s ^{1/2})		R _{film} (Ω)		CPE _{film} (S*s ^α)		α		Goodness of Fit
LiCoO ₂ -0h-Anode	5.00E+04	0.00E+00	2.27E-07	2.23E-07	3.01E+09	1.08E+08	1.26E-11	4.16E-12	9.38E-01	3.04E-02	8.06E-02
LiCoO ₂ -0h-Cathode	5.00E+04	0.00E+00			3.21E+09	2.17E+08	1.42E-11	1.59E-12	9.21E-01	9.87E-03	8.84E-02

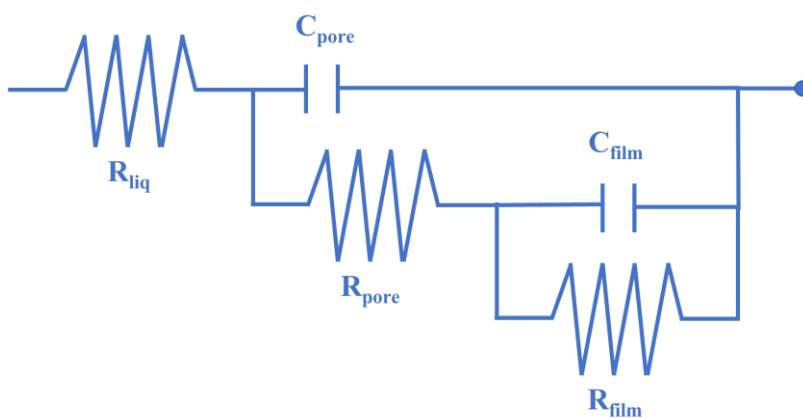


Figure 4.18 Equivalent electrical circuit to DLC film.

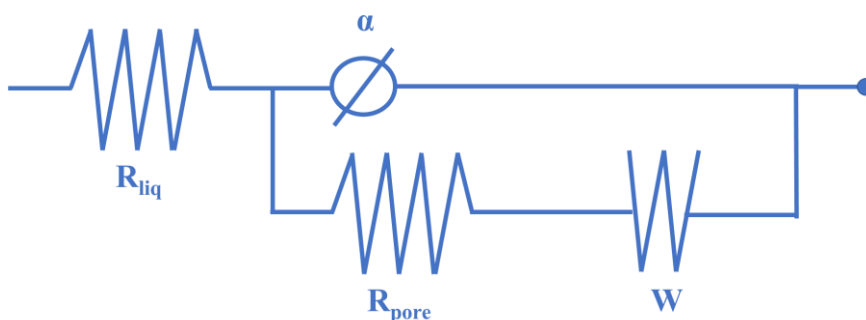


Figure 4.19 Equivalent electrical circuit to LiCoO₂ when it behaves like an anode.

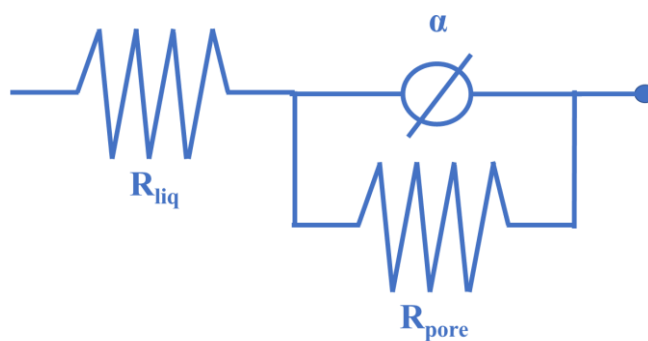


Figure 4.20 Equivalent electrical circuit to LiCoO_2 when it behaves like a cathode.

5 CONCLUSIONS AND FUTURE WORK

5.1 Conclusions

The study involved in the realization of this dissertation arises with the objective of understanding how LIB's can contribute to increase energy efficiency and, consequently, how can contribute to the energy transition.

In addition to the study of the current energy paradigm, this dissertation addresses the evolution of these batteries, the characteristics of the existing solutions and the most frequent applications of the solutions mentioned.

In the practical part of this dissertation, it was intended to study the lithium battery that was presented to be the most promising and used. However, in terms of deposition, it was necessary to study first the optimization of a traditional cathode.

The main objective of the present work was to develop DLC and LiCoO₂ coatings by MS, in order to able to work as anode and cathode respectively. The films were later characterized by several techniques.

Through SEM, was obtain a microscopic image of the DLC surface of LiCoO₂. These images permit the visualization of the morphology and porosity of the DLC. The DLC coating exhibited a columnar morphology. However, the image of the LiCoO₂ surface was not as clear as intended.

It was also possible to determine the DLC thickness in cross-section (260 nm), however the LiCoO₂ film thickness was below the detection limit of the equipment, and it was not possible to determine the film thickness by this technique, which was then obtained from AFM. From AFM analysis it was possible to estimate a LiCoO₂ thicknesses around 40 nm.

On its turn, the EDS technique allowed to measure the composition of the LiCoO₂ film deposited; however, impurities were found and could not be 100% explained.

Through the XRD it was possible to assess that both films have an amorphous structure.

Finally, corrosion tests were performed through EIS and PP. Initially, PPs were performed in DLC and LiCoO₂ coatings obtaining an E_{corr} -188 and -246mV, respectively, concluding that both coatings are resistant to corrosion. After, EIS was performed to understand the working process of the deposited films in a charge and discharge process, i.e., measuring the regions

where the coatings behave like an anode and as a cathode. The results of this method allowed to conclude that both thin films are corroded at the same rate.

To sum up everything that has been stated so far, both materials work properly and have achieved good results as a cathode and an anode, so they can both be used as thin films for batteries.

5.2 Notes and potentially useful elements

In the future is necessary to try other deposition technique to increase the deposition rate and optimize the thickness of the LiCoO_2 film. Furthermore, is also important to understand the reason of the impurities in the LiCoO_2 film chemical characterization.

In another perspective, it would be interesting to quantify the environmental impacts of the life cycle of the battery that is intended to be built on this project and compare the various impacts of the different phases for various types of batteries.

The perfect solution for energy storage doesn't exist, even so it's necessary to improve the existent solutions and investigate new ones.

BIBLIOGRAPHIC REFERENCES

- Administration, U. S. E. I., 1000 Independence Ave., S., & Washington, D. 20585. (2023). *Glossary - U.S. Energy Information Administration (EIA)*. <https://www.eia.gov/tools/glossary/>
- Bernal-Agustín, J. L., & Dufo-López, R. (2009). *Simulation and optimization of stand-alone hybrid renewable energy systems*. *Renewable and Sustainable Energy Reviews*. <https://doi.org/10.1016/j.rser.2009.01.010>
- Blomgren, G. E. (2017). The development and future of lithium ion batteries. *J. Electrochem. Soc.*, *164*(1), A5019-5025. <https://doi.org/10.1149/2.0251701jes>
- Boko, M., Niang, I., Nyong, A., Vogel, C., Githeko, A., Medany, M., Osman-Elasha, B., Tabo, R., Yanda, P., Dubois, G., wa Githendu, M., Hilmi, K., Misselhorn, A., Ziervogel, G., Semmazzi, F., Senouci, M., Niang, I., Nyong, A., Vogel, C., ... Hanson, C. (2007). Africa Coordinating Lead Authors: Lead Authors: Review Editors: This chapter should be cited as. In *Climate Change*.
- Botto, R. E. (2007). *Fossil Fuels*. *EMagRes*. <https://doi.org/10.1002/9780470034590.emrstm0175>
- Breeze, P. (2014). Power System Energy Storage Technologies. *Power Generation Technologies*, 195–221. <https://doi.org/10.1016/B978-0-08-098330-1.00010-7>
- Buchmann, I. (2019). *BU-205: Types of Lithium-ion - Battery University*. Battery University. <https://batteryuniversity.com/article/bu-205-types-of-lithium-ion>
- Calderon Velasco, S., Cavaleiro, A., & Carvalho, S. (2016). Functional properties of ceramic-Ag nanocomposite coatings produced by magnetron sputtering. *Progress in Materials Science*, *84*, 158–191. <https://doi.org/10.1016/J.PMATSCI.2016.09.005>
- Carvalho, I., Dias, N., Henriques, M., Calderon V, S., Ferreira, P., Cavaleiro, A., & Carvalho, S. (2020). Antibacterial Effects of Bimetallic Clusters Incorporated in Amorphous Carbon for Stent Application. *ACS Applied Materials and Interfaces*, *12*(22), 24555–24563. <https://doi.org/10.1021/acsami.0c02821>
- Chapter 11 - Bioactive Surface Coatings for Enhancing Osseointegration of Dental Implants*. (2019). <https://www.sciencedirect.com/science/article/pii/B9780081021965000112>
- Corrosionpedia. (2019). *What is Potentiodynamic? - Definition from Corrosionpedia*. <https://www.corrosionpedia.com/definition/911/potentiodynamic>
- Crompton, T. R. (1996). Battery reference book — Second Edition. *Fuel and Energy Abstracts*, *37*(3), 192. [https://doi.org/10.1016/0140-6701\(96\)88678-4](https://doi.org/10.1016/0140-6701(96)88678-4)

-
- Dr Anand Bhatt. (2016). *How do batteries power our phones, computers and other devices?* Australian Academy of Science. <https://www.science.org.au/curious/technology-future/batteries>
- Duan, H., Xu, H., Wu, Q., Zhu, L., Zhang, Y., Yin, B., & He, H. (2023). Silicon/Graphite/Amorphous Carbon as Anode Materials for Lithium Secondary Batteries. *Molecules*, 28(2). <https://doi.org/10.3390/molecules28020464>
- Dudney, N. J. (2013). Thin Film Micro-Batteries. *The Electrochemical Society Interface*, 1–9.
- Dutrow, B. L. (1912). *X-ray Powder Diffraction (XRD)*. https://serc.carleton.edu/research_education/geochemsheets/techniques/XRD.html
- Fergus, J. W. (2010). Recent developments in cathode materials for lithium ion batteries. In *Journal of Power Sources* (Vol. 195, Issue 4, pp. 939–954). Elsevier. <https://doi.org/10.1016/j.jpowsour.2009.08.089>
- Goodenough, J. B. (2018). How we made the Li-ion rechargeable battery. *Nature Electronics* 2018 1:3, 1(3), 204–204. <https://doi.org/10.1038/s41928-018-0048-6>
- He, W., King, M., Luo, X., Dooner, M., Li, D., & Wang, J. (2021). *Technologies and economics of electric energy storages in power systems: Review and perspective*. *Advances in Applied Energy*. <https://doi.org/10.1016/j.adapen.2021.100060>
- Holechek, J. L., Geli, H. M. E., Sawalhah, M. N., & Valdez, R. (2022). A Global Assessment: Can Renewable Energy Replace Fossil Fuels by 2050? *Sustainability (Switzerland)*, 14(8). <https://doi.org/10.3390/su14084792>
- IEA. (2022). *World Energy Outlook 2022 shows the global energy crisis can be a historic turning point towards a cleaner and more secure future*. <https://www.iea.org/news/world-energy-outlook-2022-shows-the-global-energy-crisis-can-be-a-historic-turning-point-towards-a-cleaner-and-more-secure-future>
- Jung, C.-H., Shim, H., Eum, D., & Hong, S.-H. (2020). Challenges and recent progress in LiNi_xCo_yMn_{1-x-y}O₂ (NCM) cathodes for lithium ion batteries. *Journal of the Korean Ceramic Society* 2020 58:1, 58(1), 1–27. <https://doi.org/10.1007/S43207-020-00098-X>
- Kelly, P. J., & Arnell, R. D. (2000). Magnetron sputtering: a review of recent developments and applications. *Vacuum*, 56(3), 159–172. [https://doi.org/10.1016/S0042-207X\(99\)00189-X](https://doi.org/10.1016/S0042-207X(99)00189-X)
- Magar, H. S., Hassan, R. Y. A., & Mulchandani, A. (2021). Electrochemical impedance spectroscopy (Eis): Principles, construction, and biosensing applications. In *Sensors* (Vol. 21, Issue 19). <https://doi.org/10.3390/s21196578>
- Marco Tedesco. (2023). *The Paradox of Lithium*.
-

<https://news.climate.columbia.edu/2023/01/18/the-paradox-of-lithium/>

Martins, F., Moura, P., & de Almeida, A. T. (2022). The Role of Electrification in the Decarbonization of the Energy Sector in Portugal. *Energies*, 15(5). <https://doi.org/10.3390/en15051759>

Mattox, D. M. (2007). *Handbook of Physical Vapor Deposition (PVD) Processing*. Handbook of Physical Vapor Deposition (PVD) Processing. <https://doi.org/10.1016/c2009-0-18800-1>

Mikael Hanicke, Dina Ibrahim, Sören Jautelat, Martin Linder, Patrick Schaufuss, Lukas Torscht, A. van de R. (2023). *Battery 2030: Resilient, sustainable, and circular*. <https://www.mckinsey.com/industries/automotive-and-assembly/our-insights/battery-2030-resilient-sustainable-and-circular>

NanoAndMore. (2022). *What is Atomic Force Microscopy (AFM)*. NanoAndMore. <https://www.nanoandmore.com/what-is-atomic-force-microscopy>

Nitta, N., Wu, F., Lee, J. T., & Yushin, G. (2015). Li-ion battery materials: Present and future. *Materials Today*, 18(5), 252–264. <https://doi.org/10.1016/j.mattod.2014.10.040>

Noh, J. P., Cho, G. B., Jung, K. T., Kang, W. G., Ha, C. W., Ahn, H. J., Ahn, J. H., Nam, T. H., & Kim, K. W. (2012). Fabrication of LiCoO₂ thin film cathodes by DC magnetron sputtering method. In *Materials Research Bulletin* (Vol. 47, Issue 10, pp. 2823–2826). <https://doi.org/10.1016/j.materresbull.2012.04.065>

Nzereogu, P. U., Omah, A. D., Ezema, F. I., Iwuoha, E. I., & Nwanya, A. C. (2022). Anode materials for lithium-ion batteries: A review. *Applied Surface Science Advances*, 9, 100233. <https://doi.org/10.1016/J.APSADV.2022.100233>

Parliament, E. (2020). *A European Green Deal*. New Circular Economy Action Plan. https://commission.europa.eu/strategy-and-policy/priorities-2019-2024/european-green-deal_en%0Ahttps://ec.europa.eu/info/strategy/priorities-2019-2024/european-green-deal_en

Patil, A., Patil, V., Wook Shin, D., Choi, J. W., Paik, D. S., & Yoon, S. J. (2008). Issue and challenges facing rechargeable thin film lithium batteries. In *Materials Research Bulletin* (Vol. 43, Issues 8–9, pp. 1913–1942). <https://doi.org/10.1016/j.materresbull.2007.08.031>

Peng, M., Shin, K., Jiang, L., Jin, Y., Zeng, K., Zhou, X., & Tang, Y. (2022). Alloy-Type Anodes for High-Performance Rechargeable Batteries. *Angewandte Chemie International Edition*, 61(33), e202206770. <https://doi.org/10.1002/ANIE.202206770>

Qi, Z., & Wang, H. (2020). Advanced Thin Film Cathodes for Lithium Ion Batteries. *Research*, 2020, 1–24. <https://doi.org/10.34133/2020/2969510>

-
- Richards, W. D., Miara, L. J., Wang, Y., Kim, J. C., & Ceder, G. (2016). Interface Stability in Solid-State Batteries. *Chemistry of Materials*, 28(1), 266–273. <https://doi.org/10.1021/acs.chemmater.5b04082>
- RTI Laboratories. (2020). *SEM/EDS Analysis*. Techniques. <https://rtilab.com/techniques/sem-ed-s-analysis/>
- Scrosati, B. (2011). History of lithium batteries. *Journal of Solid State Electrochemistry*, 15(7–8), 1623–1630. <https://doi.org/10.1007/s10008-011-1386-8>
- Scrosati, B., & Garche, J. (2010). Lithium batteries: Status, prospects and future. *Journal of Power Sources*, 195(9), 2419–2430. <https://doi.org/10.1016/j.jpowsour.2009.11.048>
- Sorting Hat Technologies Pvt Ltd. (2023). *Time Constant*. <https://unacademy.com/content/jee/study-material/physics/time-constant/>
- Stan, A.-I., Maciej, M., Maciej, swierczyński, M., Stroe, D.-I., Teodorescu, R., & Andreasen, S. J. (2014). Lithium ion battery chemistries from renewable energy storage to automotive and back-up power applications — An overview. In *2014 International Conference on Optimization of Electrical and Electronic Equipment (OPTIM)*. <https://doi.org/10.1109/OPTIM.2014.6850936>
- Stan, A. I., Swierczynski, M., Stroe, D. I., Teodorescu, R., & Andreasen, S. J. (2014). Lithium ion battery chemistries from renewable energy storage to automotive and back-up power applications - An overview. *2014 International Conference on Optimization of Electrical and Electronic Equipment, OPTIM 2014*, 713–720. <https://doi.org/10.1109/OPTIM.2014.6850936>
- Takada, K. (2013). Progress and prospective of solid-state lithium batteries. *Acta Materialia*, 61(3), 759–770. <https://doi.org/10.1016/j.actamat.2012.10.034>
- The Growing Role of Minerals and Metals for a Low Carbon Future. (2017). In *The Growing Role of Minerals and Metals for a Low Carbon Future*. <https://doi.org/10.1596/28312>
- USGS.gov | *Science for a changing world*. (2010). <https://www.usgs.gov/>
- Wang, Yixu, & Huang, H. Y. S. (2011). Comparison of lithium-ion battery cathode materials and the internal stress development. *ASME 2011 International Mechanical Engineering Congress and Exposition, IMECE 2011*, 4(PARTS A AND B), 1685–1694. <https://doi.org/10.1115/imece2011-65663>
- Wang, Yuxing, Liu, B., Li, Q., Cartmell, S., Ferrara, S., Deng, Z. D., & Xiao, J. (2015a). Lithium and lithium ion batteries for applications in microelectronic devices: A review. In *Journal of Power Sources* (Vol. 286, pp. 330–345). Elsevier. <https://doi.org/10.1016/j.jpowsour.2015.03.164>
-

- Wang, Yuxing, Liu, B., Li, Q., Cartmell, S., Ferrara, S., Deng, Z. D., & Xiao, J. (2015b). Lithium and lithium ion batteries for applications in microelectronic devices: A review. In *Journal of Power Sources* (Vol. 286, Issue 15, pp. 330–345). Elsevier. <https://doi.org/10.1016/j.jpowsour.2015.03.164>
- Yi, T.-F., Jiang, L.-J., Shu, J., Yue, C.-B., Zhu, R.-S., & Qiao, H.-B. (2010). Recent development and application of Li₄Ti₅O₁₂ as anode material of lithium ion battery. *Journal of Physics and Chemistry of Solids*, 71(9), 1236–1242. <https://doi.org/10.1016/j.jpocs.2010.05.001>
- Yildiz, L. (2018). *Fossil Fuels*. Comprehensive Energy Systems. <https://doi.org/10.1016/B978-0-12-809597-3.00111-5>
- Yoshio, M., Brodd, R. J., & Kozawa, A. (2009). Lithium-ion batteries: Science and technologies. *Lithium-Ion Batteries: Science and Technologies*, 1–452. <https://doi.org/10.1007/978-0-387-34445-4>
- Zablocki, A. (2019). *Energy Storage | Energy Storage*.
- Zhou, Y. N., Xue, M. Z., & Fu, Z. W. (2013). Nanostructured thin film electrodes for lithium storage and all-solid-state thin-film lithium batteries. *Journal of Power Sources*, 234, 310–332. <https://doi.org/10.1016/j.jpowsour.2013.01.183>